Supplementary Materials

Influence of an Electric-field on the Topological Stability of the Neutral Lithium Dimer

Xinxin Feng[1], Alireza Azizi[2], Tianlv Xu[1], Wenjing Yu[1], Xiaopeng Mi[1], Hui Lu[1], Herbert Früchtl[3], Tanja van Mourik[3], Steven R. Kirk[*1] and Samantha Jenkins[*1]

[1]Key Laboratory of Chemical Biology and Traditional Chinese Medicine Research and Key Laboratory of Resource National and Local Joint Engineering Laboratory for New Petro-chemical Materials and Fine Utilization of Resources, College of Chemistry and Chemical Engineering, Hunan Normal University, Changsha, Hunan 410081, China

[2]State Key Laboratory of Powder Metallurgy, School of Materials Science & Engineering, Central South University, Changsha, Hunan 410083, China

[3]EaStCHEM School of Chemistry, University of Saint Andrews, North Haugh, St Andrews, Fife KY16 9ST, Scotland, United Kingdom.

Email : steven.kirk@cantab.net
Email : samanthajsuman@gmail.com

1. Supplementary Materials S1. NG-QTAIM and stress tensor theoretical background.

2. Supplementary Materials S2. Hessian of $\rho(\mathbf{r})$ lithium $\{\boldsymbol{q,q'}\}$ and $\{\boldsymbol{p,p'}\}$ path-packets.

3. Supplementary Materials S3. Variation of the Hessian stress tensor ellipticity $\varepsilon_{\sigma H}$ profile along the Li1-Li2 bond-path.

4. Supplementary Materials S4. Stress tensor $\boldsymbol{\sigma}(\mathbf{r})$ eigenvectors subjected to an electric field.

5. Supplementary Materials S5. Hessian of $\rho(\mathbf{r})$ eigenvectors subjected to an electric field.

6. Supplementary Materials S6. Stress tensor lithium $\{\boldsymbol{p_\sigma,p'_\sigma}\}$ path-packets.

7. Supplementary Materials S7. Hessian of $\rho(\mathbf{r})$ partitioning scheme scalar QTAIM measures.

8. Supplementary Materials S8. Critical point separations for neutral Li_2 subjected to an electric field.

9. Supplementary Materials S9. Stretched neutral Li_2 for the Hessian of $\rho(\mathbf{r})$ and stress tensor $\boldsymbol{\sigma}(\mathbf{r})$.

1. Supplementary Materials S1.

I(i) *QTAIM and stress tensor bond critical point (BCP) properties; ellipticity ε:*

The four types of QTAIM critical points are labeled using the notation (R, ω) where R is the rank of the Hessian matrix, i.e., the number of distinct non-zero eigenvalues and ω is the signature (the algebraic sum of the signs of the eigenvalues); the (3, -3) [nuclear critical point (*NCP*), a local maximum], (3, -1) and (3, 1) [saddle points, referred to as bond critical points (*BCP*) and ring critical points (*RCP*), respectively] and (3, 3) [the cage critical points (*CCP*)]. In the limit that the forces on the nuclei are zero, an atomic interaction line[1], the line passing through a *BCP* and terminating on two nuclear attractors along which the charge density $\rho(\mathbf{r})$ is locally maximal with respect to nearby lines, becomes a bond-path[2]. The full set of critical points with the bond-paths of a molecule or cluster is referred to as the molecular graph.

- Ellipticity $\varepsilon = |\lambda_1|/|\lambda_2| - 1$.

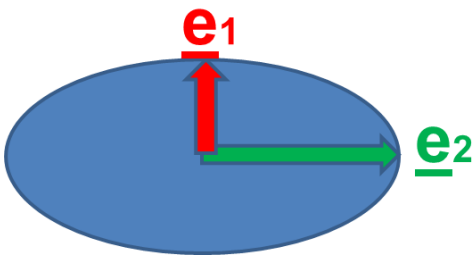

Scheme S1. The cross section through a bond at the bond critical point (*BCP*). The λ_1 and λ_2 eigenvalues with associated eigenvectors $\underline{\mathbf{e}}_1$ and $\underline{\mathbf{e}}_2$ respectively, define the axes of the ellipse and indicate the magnitudes of the least and greatest extents of the distribution of $\rho(\mathbf{r})$.

The ellipticity, ε, defined as $\varepsilon = |\lambda_1|/|\lambda_2| - 1$, quantifies the relative accumulation of the electronic charge density $\rho(\mathbf{r_b})$ distribution in the two directions $\underline{\mathbf{e}}_1$ and $\underline{\mathbf{e}}_2$ that are perpendicular to the bond-path at a Bond Critical Point (*BCP*) with position $\mathbf{r_b}$. For ellipticity $\varepsilon > 0$, the shortest and longest axes of the elliptical distribution of $\rho(\mathbf{r_b})$ are associated with the λ_1 and λ_2 eigenvalues, respectively. From the electron-preceding perspective a change in the electronic charge density distribution that defines a chemical bond causes in a change in atomic positions[3]. Bone and Bader later proposed that the direction of motion of the atoms that results from a slightly perturbed structure coincides with the direction of motion of the electrons[4–6].

I(ii). *QTAIM bond-path properties; bond-path length (BPL), bond-path curvature and the stress tensor eigenvalue* $\lambda_{3\sigma}$ *:*

The bond-path length (BPL) is defined as the length of the path traced out by the $\underline{\mathbf{e}}_3$ eigenvector of the Hessian of the total charge density $\rho(\mathbf{r})$, passing through the *BCP*, along which $\rho(\mathbf{r})$ is locally maximal with respect to any neighboring paths. The bond-path curvature separating two bonded nuclei is defined as the dimensionless ratio (BPL - GBL)/GBL, where the BPL is defined to be the bond-path length associated and GBL is the inter-nuclear separation. The BPL often exceeds the GBL particularly in strained bonding environments[5]. Earlier, one of the current authors hypothesized that a bond-path may possess 1-D, 2-D or

a 3-D morphology[7], with 2-D or a 3-D bond-paths associated with a *BCP* with ellipticity $\varepsilon > 0$, being due to the differing degrees of charge density accumulation, of the λ_2 and λ_1 eigenvalues respectively. Bond-paths possessing zero and non-zero values of the bond-path curvature defined by equation **(2)** can be considered to possess 1-D and 2-D topologies respectively. We start by choosing the length traced out in 3-D by the path swept by the tips of the scaled $\underline{\mathbf{e}}_2$ eigenvectors of the λ_2 eigenvalue, the scaling factor being chosen as the ellipticity ε, see **Scheme S1 (a)**.

- Stress tensor eigenvalue $\lambda_{3\sigma}$

This is used as a measure of bond-path instability, for values of $\lambda_{3\sigma} < 0$ and is calculated within the QTAIM partitioning.

The quantum stress tensor $\boldsymbol{\sigma}(\mathbf{r})$ is directly related to the Ehrenfest force by the virial theorem and therefore provides a physical explanation of the low frequency normal modes that accompany structural rearrangements[8]. In this work we use the definition of the stress tensor proposed by Bader to investigate the stress tensor properties within QTAIM[9]. The quantum stress tensor $\boldsymbol{\sigma}(\mathbf{r})$ is used to characterize the mechanics of the forces acting on the electron density distribution in open systems, defined as:

$$\boldsymbol{\sigma}(\mathbf{r}) = -\frac{1}{4}\left[\left(\frac{\partial^2}{\partial \mathbf{r}_i \partial \mathbf{r}'_j} + \frac{\partial^2}{\partial \mathbf{r}'_i \partial \mathbf{r}_j} - \frac{\partial^2}{\partial \mathbf{r}_i \partial \mathbf{r}_j} - \frac{\partial^2}{\partial \mathbf{r}'_i \partial \mathbf{r}'_j}\right) \cdot \gamma(\mathbf{r}, \mathbf{r}')\right]_{\mathbf{r}=\mathbf{r}'} \qquad \textbf{(2)}$$

Where $\gamma(\mathbf{r},\mathbf{r}')$ is the one-body density matrix,

$$\gamma(\mathbf{r}, \mathbf{r}') = N \int \Psi(\mathbf{r}, \mathbf{r}_2, \ldots, \mathbf{r}_N)\Psi^*(\mathbf{r}', \mathbf{r}_2, \ldots, \mathbf{r}_N)\mathrm{d}\mathbf{r}_2 \cdots \mathrm{d}\mathbf{r}_N \qquad \textbf{(3)}$$

The stress tensor is then any quantity $\boldsymbol{\sigma}(\mathbf{r})$, that satisfies equation **(2)** since one can add any divergence free tensor to the stress tensor without violating this definition[9–11].

Earlier, it was found that the stress tensor trajectories $\mathbb{T}_\sigma(s)$ were in line with physical intuition[12].

If we first consider a tiny cube of fluid flowing in 3-D space the stress $\Pi(x, y, z, t)$, a rank-3 tensor field, has nine components[13] of these the three diagonal components Π_{xx}, Π_{yy}, and Π_{zz} correspond to normal stress. A negative value for these normal components signifies a compression of the cube, conversely a positive value refers to pulling or tension, where more negative/positive values correspond to increased compression/tension of the cube. Diagonalization of the stress tensor $\boldsymbol{\sigma}(\mathbf{r})$, returns the principal electronic stresses Π_{xx}, Π_{yy}, and Π_{zz} that are realized as the stress tensor eigenvalues $\lambda_{1\sigma}$, $\lambda_{2\sigma}$, $\lambda_{3\sigma}$, with corresponding eigenvectors $\underline{\mathbf{e}}_{1\sigma}$, $\underline{\mathbf{e}}_{2\sigma}$, $\underline{\mathbf{e}}_{3\sigma}$ are calculated within the QTAIM partitioning.

Previously, $\lambda_{3\sigma}$ was used to detect the lowering of the symmetry, caused by a torsion about the central C-C bond in biphenyl, inducing a phase transition[8]. The *BCP*s calculated with QTAIM and stress tensor partitionings will not always coincide, particularly under the application of external force, such as an applied torsion.

2. Supplementary Materials S2. Hessian of $\rho(\mathbf{r})$ lithium {***q,q′***} and {***p,p ′***} path-packets.

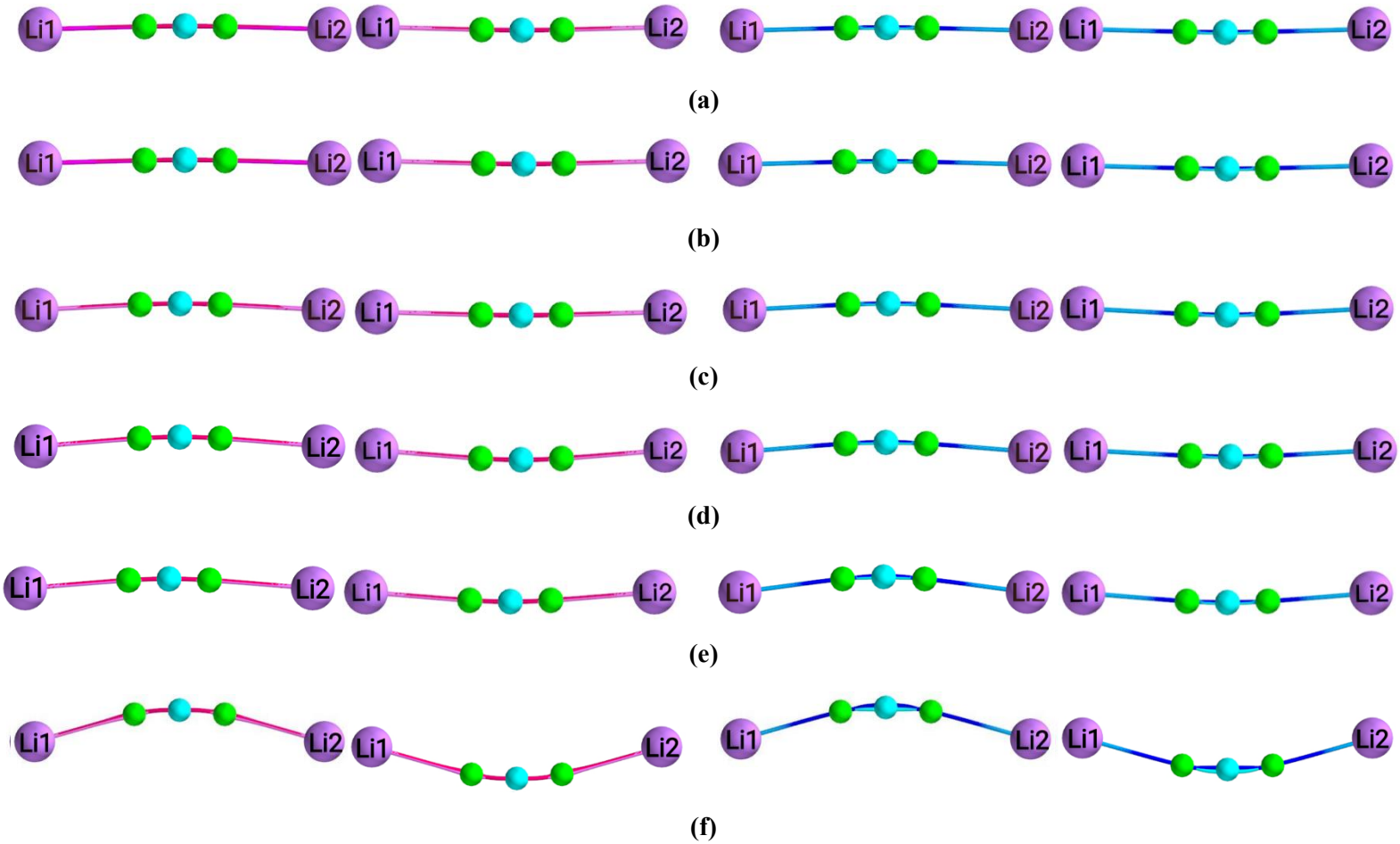

Figure S2(a). The Hessian of $\rho(\mathbf{r})$ lithium molecular graphs displaying the Hessian of $\rho(\mathbf{r})$ lithium {***q,q′***} (left pair of panels) and {***p,p ′***} (right panel of panels) path-packets for values of the external electric field, $\mathbf{E}_y$-field (in a.u.) = $\pm 20.0\text{x}10^{-4}$, $\pm 40.0\text{x}10^{-4}$, $\pm 60.0\text{x}10^{-4}$, $\pm 80.0\text{x}10^{-4}$, $\pm 100.0\text{x}10^{-4}$, are provided in left ($+\mathbf{E}_y$) and right ($-\mathbf{E}_y$) panels of sub-figures **(a-f)** respectively, see **Scheme 1** electric field directions.

.

3. Supplementary Materials S3. Variation of the Hessian stress tensor ellipticity $\varepsilon_{\sigma H}$ profile along the Li1-Li2 bond-path

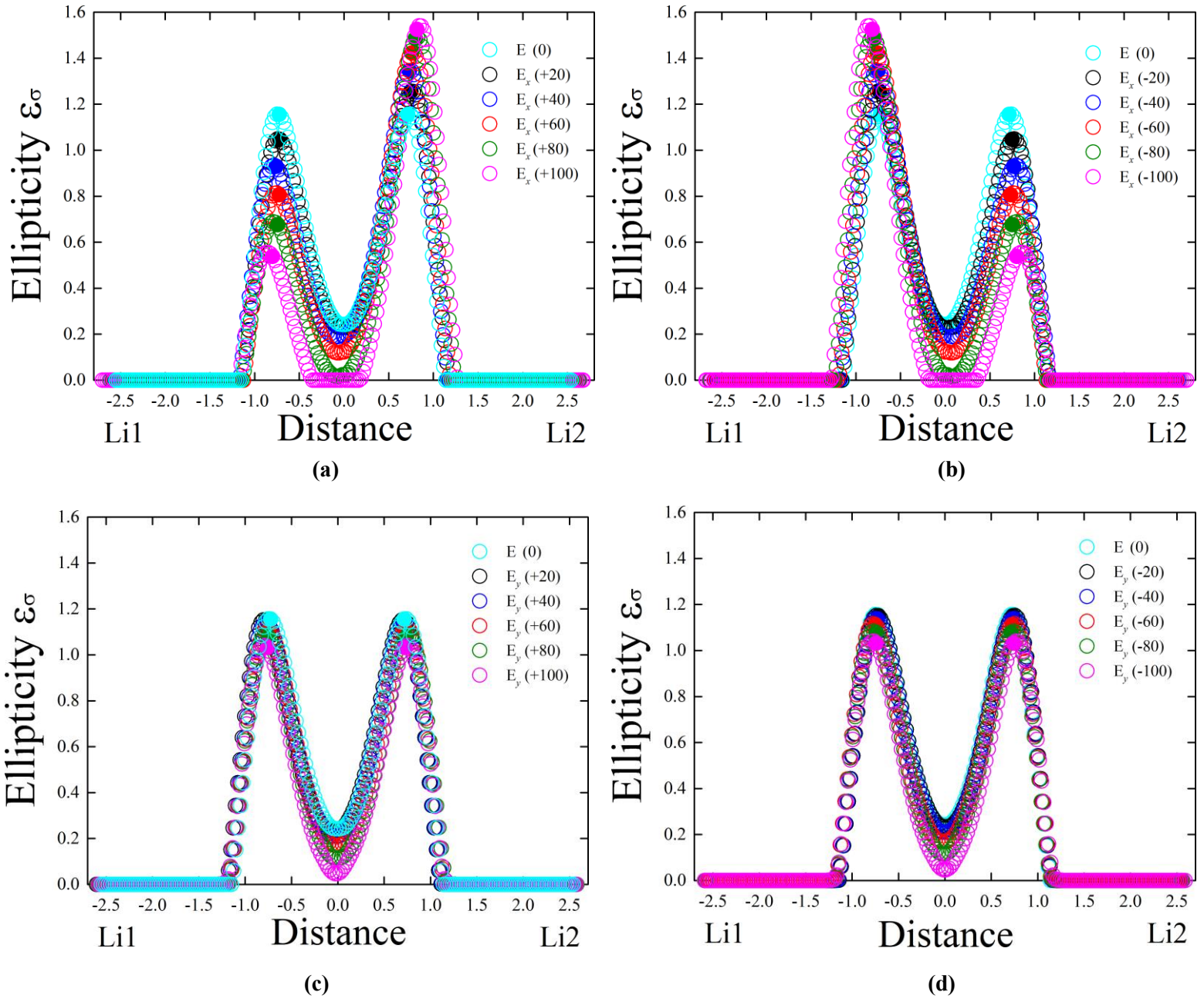

Figure S3. The variation of the Hessian stress tensor ellipticity $\varepsilon_{\sigma H} = |\lambda_{1\sigma}|/|\lambda_{2\sigma}| - 1$ profile with distance along the Li-*BCP*-*NNA*-*BCP*-Li separation in a.u. for the neutral lithium molecule Li_2 cluster. In the *NNA* is located at a distance = 0.0 in an electric field at $\mathbf{E}_x$-field (in a.u.) = 0, $+20.0\times10^{-4}$, $+40.0\times10^{-4}$, $+60.0\times10^{-4}$, $+80.0\times10^{-4}$, $+100.0\times10^{-4}$ and $\mathbf{E}_x$-field (in a.u) = 0, -20.0×10^{-4}, -40.0×10^{-4}, -60.0×10^{-4}, -80.0×10^{-4}, -100.0×10^{-4} are presented in sub-figures **(a-b)** respectively. The corresponding results for the $\pm\mathbf{E}_y$-field are provided in sub-figures **(c-d)** respectively.

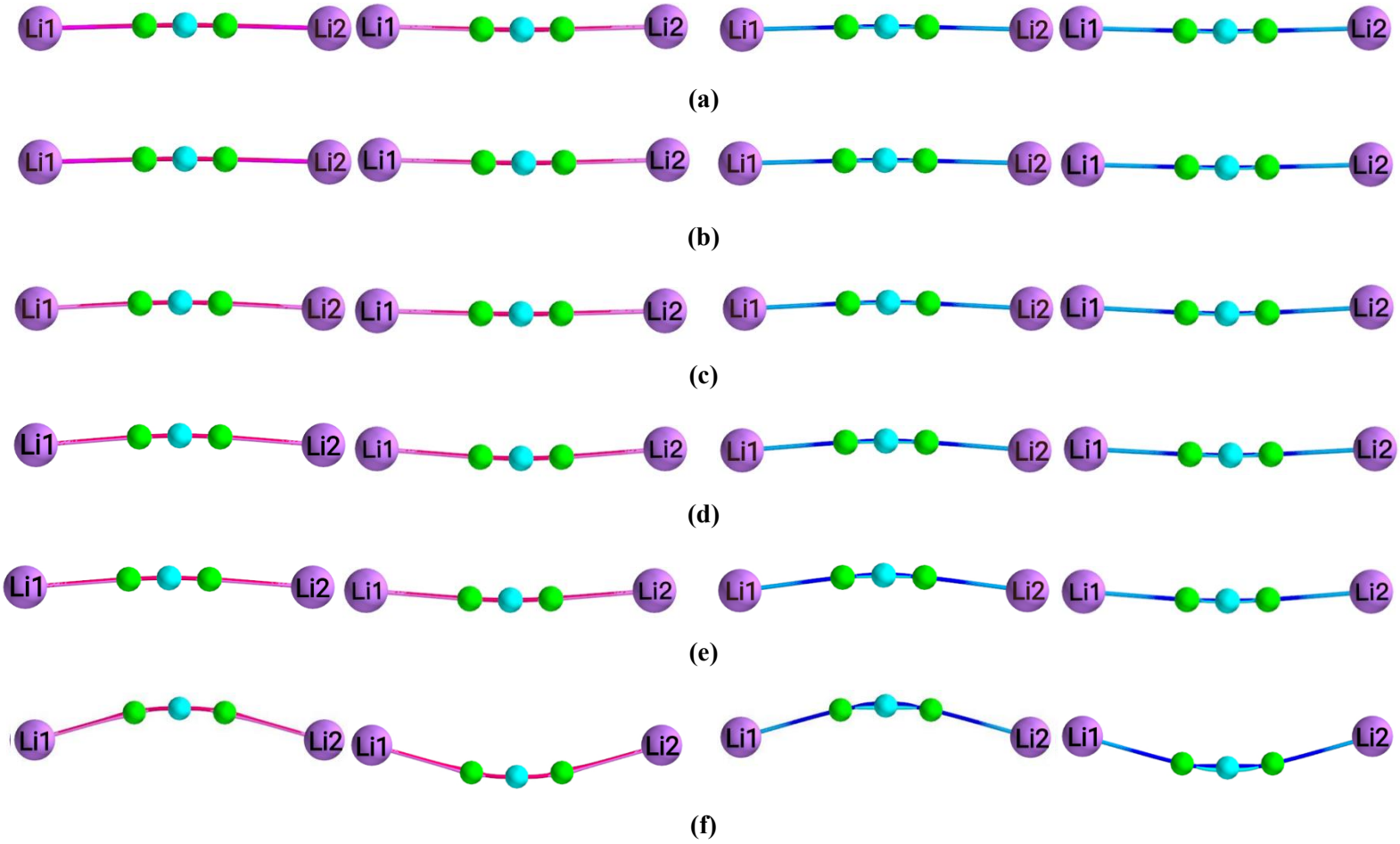

Figure S3(b). The view of the Hessian of $\rho(\mathbf{r})$ lithium molecular graphs displaying the $\{q,q'\}$ path-packets for values of the external electric field, $\mathbf{E}_z$-field (in a.u.) = $\pm 20.0\text{x}10^{-4}$, $\pm 40.0\text{x}10^{-4}$, $\pm 60.0\text{x}10^{-4}$, $\pm 80.0\text{x}10^{-4}$, $\pm 100.0\text{x}10^{-4}$, are provided in left ($+\mathbf{E}_z$) and right ($-\mathbf{E}_z$) panels of sub-figures **(a-f)** respectively, see **Figure S3(a)** for further details.

4. Supplementary Materials S4. Stress tensor **σ**(**r**) eigenvectors subjected to an electric field.

Table S4(a). The stress tensor **σ**(**r**) eigenvectors $\{\underline{\mathbf{e}}_{1\sigma}, \underline{\mathbf{e}}_{2\sigma}, \underline{\mathbf{e}}_{3\sigma}\}$ for the $\mathbf{E}_x$-field (in a.u.) of the (Li-Li) molecules. The *x*-axis is aligned with the bond-path in each case for all entries in **Table S4(a)-Table S4(d)**. Note, for **E**-field = -144 there is only an Li1-Li2 *BCP.* A multiplication factor of $x10^{-4}$ for the **E**-field should be used for all entries in **Supplementary Materials S4**.

$\mathbf{E}_x$-field	Eigen-Vectors	*BCP*(Li1-*NNA*3) (*x*, *y*, *z*)	*BCP*(Li2-*NNA*3) (*x*, *y*, *z*)
0	$\underline{\mathbf{e}}_{1\sigma}$	(1.000, 0.000, 0.000)	(1.000, 0.000, 0.000)
0	$\underline{\mathbf{e}}_{2\sigma}$	(0.000, 1.000, 0.000)	(0.000, 1.000, 0.000)
0	$\underline{\mathbf{e}}_{3\sigma}$	(0.000, 0.000, 1.000)	(0.000, 0.000, 1.000)
-20	$\underline{\mathbf{e}}_{1\sigma}$	(1.000, 0.000, 0.000)	(1.000, 0.000, 0.000)
-20	$\underline{\mathbf{e}}_{2\sigma}$	(0.000, 1.000, 0.000)	(0.000, 0.000, 1.000)
-20	$\underline{\mathbf{e}}_{3\sigma}$	(0.000, 0.000, 1.000)	(0.000, 1.000, 0.000)
-40	$\underline{\mathbf{e}}_{1\sigma}$	(1.000, 0.000, 0.000)	(1.000, 0.000, 0.000)
-40	$\underline{\mathbf{e}}_{2\sigma}$	(0.000, 0.000, 1.000)	(0.000, 0.000, 1.000)
-40	$\underline{\mathbf{e}}_{3\sigma}$	(0.000, 1.000, 0.000)	(0.000, 1.000, 0.000)
-60	$\underline{\mathbf{e}}_{1\sigma}$	(1.000, 0.000, 0.000)	(1.000, 0.000, 0.000)
-60	$\underline{\mathbf{e}}_{2\sigma}$	(0.000, 0.000, 1.000)	(0.000, 1.000, 0.000)
-60	$\underline{\mathbf{e}}_{3\sigma}$	(0.000, 1.000, 0.000)	(0.000, 0.000, 1.000)
-80	$\underline{\mathbf{e}}_{1\sigma}$	(1.000, 0.000, 0.000)	(1.000, 0.000, 0.000)
-80	$\underline{\mathbf{e}}_{2\sigma}$	(0.000, 1.000, 0.000)	(0.000, 1.000, 0.000)
-80	$\underline{\mathbf{e}}_{3\sigma}$	(0.000, 0.000, 1.000)	(0.000, 0.000, 1.000)
-100	$\underline{\mathbf{e}}_{1\sigma}$	(1.000, 0.000, 0.000)	(0.000, 0.000, 1.000)
-100	$\underline{\mathbf{e}}_{2\sigma}$	(0.000, 0.000, 1.000)	(0.000, 1.000, 0.000)
-100	$\underline{\mathbf{e}}_{3\sigma}$	(0.000, 1.000, 0.000)	(1.000, 0.000, 0.000)
-110	$\underline{\mathbf{e}}_{1\sigma}$	(1.000, 0.000, 0.000)	(0.000, 0.000, 1.000)
-110	$\underline{\mathbf{e}}_{2\sigma}$	(0.000, 0.000, 1.000)	(0.000, 1.000, 0.000)
-110	$\underline{\mathbf{e}}_{3\sigma}$	(0.000, 1.000, 0.000)	(1.000, 0.000, 0.000)
-120	$\underline{\mathbf{e}}_{1\sigma}$	(1.000, 0.000, 0.000)	(0.000, 0.000, 1.000)
-120	$\underline{\mathbf{e}}_{2\sigma}$	(0.000, 0.000, 1.000)	(0.000, 1.000, 0.000)
-120	$\underline{\mathbf{e}}_{3\sigma}$	(0.000, 1.000, 0.000)	(1.000, 0.000, 0.000)
-130	$\underline{\mathbf{e}}_{1\sigma}$	(1.000, 0.000, 0.000)	(0.000, 1.000, 0.000)
-130	$\underline{\mathbf{e}}_{2\sigma}$	(0.000, 1.000, 0.000)	(0.000, 0.000, 1.000)
-130	$\underline{\mathbf{e}}_{3\sigma}$	(0.000, 0.000, 1.000)	(1.000, 0.000, 0.000)
-140	$\underline{\mathbf{e}}_{1\sigma}$	(1.000, 0.000, 0.000)	(0.000, 1.000, 0.000)
-140	$\underline{\mathbf{e}}_{2\sigma}$	(0.000, 1.000, 0.000)	(0.000, 0.000, 1.000)
-140	$\underline{\mathbf{e}}_{3\sigma}$	(0.000, 0.000, 1.000)	(1.000, 0.000, 0.000)
-141	$\underline{\mathbf{e}}_{1\sigma}$	(1.000, 0.000, 0.000)	(0.000, 0.000, 1.000)
-141	$\underline{\mathbf{e}}_{2\sigma}$	(0.000, 0.000, 1.000)	(0.000, 1.000, 0.000)
-141	$\underline{\mathbf{e}}_{3\sigma}$	(0.000, 1.000, 0.000)	(1.000, 0.000, 0.000)
-142	$\underline{\mathbf{e}}_{1\sigma}$	(1.000, 0.000, 0.000)	(0.000, 0.000, 1.000)

-142	$\underline{\mathbf{e}}_{2\sigma}$	(0.000, 0.000, 1.000)	(0.000, 1.000, 0.000)
-142	$\underline{\mathbf{e}}_{3\sigma}$	(0.000, 1.000, 0.000)	(1.000, 0.000, 0.000)
-143	$\underline{\mathbf{e}}_{1\sigma}$	(1.000, 0.000, 0.000)	(0.000, 0.000, 1.000)
-143	$\underline{\mathbf{e}}_{2\sigma}$	(0.000, 0.000, 1.000)	(0.000, 1.000, 0.000)
-143	$\underline{\mathbf{e}}_{3\sigma}$	(0.000, 1.000, 0.000)	(1.000, 0.000, 0.000)
-144	$\underline{\mathbf{e}}_{1\sigma}$	(0.000, 1.000, 0.000)	
-144	$\underline{\mathbf{e}}_{2\sigma}$	(0.000, 0.000, 1.000)	
-144	$\underline{\mathbf{e}}_{3\sigma}$	(1.000, 0.000, 0.000)	

Table S4(b). The stress tensor $\boldsymbol{\sigma}(\mathbf{r})$ eigenvectors $\{\underline{\mathbf{e}}_{1\sigma}, \underline{\mathbf{e}}_{2\sigma}, \underline{\mathbf{e}}_{3\sigma}\}$ for the $\mathbf{E}_x$-field (in a.u.) of the (Li-Li) molecules. See **Table S4(a)** for further details. Note, for **E**-field = +144 there is only an Li1-Li2 *BCP*

$\mathbf{E}_x$-field	Eigen-Vectors	*BCP*(Li1-*NNA*3) (*x*, *y*, *z*)	*BCP*(Li2-*NNA*3) (*x*, *y*, *z*)
0	$\underline{\mathbf{e}}_{1\sigma}$	(1.000, 0.000, 0.000)	(1.000, 0.000, 0.000)
0	$\underline{\mathbf{e}}_{2\sigma}$	(0.000, 1.000, 0.000)	(0.000, 1.000, 0.000)
0	$\underline{\mathbf{e}}_{3\sigma}$	(0.000, 0.000, 1.000)	(0.000, 0.000, 1.000)
+20	$\underline{\mathbf{e}}_{1\sigma}$	(1.000, 0.000, 0.000)	(1.000, 0.000, 0.000)
+20	$\underline{\mathbf{e}}_{2\sigma}$	(0.000, 0.000, 1.000)	(0.000, 0.000, 1.000)
+20	$\underline{\mathbf{e}}_{3\sigma}$	(0.000, 1.000, 0.000)	(0.000, 1.000, 0.000)
+40	$\underline{\mathbf{e}}_{1\sigma}$	(1.000, 0.000, 0.000)	(1.000, 0.000, 0.000)
+40	$\underline{\mathbf{e}}_{2\sigma}$	(0.000, 0.000, 1.000)	(0.000, 1.000, 0.000)
+40	$\underline{\mathbf{e}}_{3\sigma}$	(0.000, 1.000, 0.000)	(0.000, 0.000, 1.000)
+60	$\underline{\mathbf{e}}_{1\sigma}$	(1.000, 0.000, 0.000)	(1.000, 0.000, 0.000)
+60	$\underline{\mathbf{e}}_{2\sigma}$	(0.000, 1.000, 0.000)	(0.000, 1.000, 0.000)
+60	$\underline{\mathbf{e}}_{3\sigma}$	(0.000, 0.000, 1.000)	(0.000, 0.000, 1.000)
+80	$\underline{\mathbf{e}}_{1\sigma}$	(1.000, 0.000, 0.000)	(1.000, 0.000, 0.000)
+80	$\underline{\mathbf{e}}_{2\sigma}$	(0.000, 1.000, 0.000)	(0.000, 1.000, 0.000)
+80	$\underline{\mathbf{e}}_{3\sigma}$	(0.000, 0.000, 1.000)	(0.000, 0.000, 1.000)
+100	$\underline{\mathbf{e}}_{1\sigma}$	(1.000, 0.000, 0.000)	(0.000, 1.000, 0.000)
+100	$\underline{\mathbf{e}}_{2\sigma}$	(0.000, 1.000, 0.000)	(0.000, 0.000, 1.000)
+100	$\underline{\mathbf{e}}_{3\sigma}$	(0.000, 0.000, 1.000)	(1.000, 0.000, 0.000)
+110	$\underline{\mathbf{e}}_{1\sigma}$	(1.000, 0.000, 0.000)	(0.000, 0.000, 1.000)
+110	$\underline{\mathbf{e}}_{2\sigma}$	(0.000, 0.000, 1.000)	(0.000, 1.000, 0.000)
+110	$\underline{\mathbf{e}}_{3\sigma}$	(0.000, 1.000, 0.000)	(1.000, 0.000, 0.000)
+120	$\underline{\mathbf{e}}_{1\sigma}$	(1.000, 0.000, 0.000)	(0.000, 1.000, 0.000)
+120	$\underline{\mathbf{e}}_{2\sigma}$	(0.000, 1.000, 0.000)	(0.000, 0.000, 1.000)
+120	$\underline{\mathbf{e}}_{3\sigma}$	(0.000, 0.000, 1.000)	(1.000, 0.000, 0.000)
+130	$\underline{\mathbf{e}}_{1\sigma}$	(1.000, 0.000, 0.000)	(0.000, 1.000, 0.000)
+130	$\underline{\mathbf{e}}_{2\sigma}$	(0.000, 1.000, 0.000)	(0.000, 0.000, 1.000)
+130	$\underline{\mathbf{e}}_{3\sigma}$	(0.000, 0.000, 1.000)	(1.000, 0.000, 0.000)
+140	$\underline{\mathbf{e}}_{1\sigma}$	(1.000, 0.000, 0.000)	(0.000, 1.000, 0.000)

+140	$\underline{\mathbf{e}}_{2\sigma}$	(0.000, 1.000, 0.000)	(0.000, 0.000, 1.000)
+140	$\underline{\mathbf{e}}_{3\sigma}$	(0.000, 0.000, 1.000)	(1.000, 0.000, 0.000)
+141	$\underline{\mathbf{e}}_{1\sigma}$	(1.000, 0.000, 0.000)	(0.000, 1.000, 0.000)
+141	$\underline{\mathbf{e}}_{2\sigma}$	(0.000, 1.000, 0.000)	(0.000, 0.000, 1.000)
+141	$\underline{\mathbf{e}}_{3\sigma}$	(0.000, 0.000, 1.000)	(1.000, 0.000, 0.000)
+142	$\underline{\mathbf{e}}_{1\sigma}$	(1.000, 0.000, 0.000)	(0.000, 1.000, 0.000)
+142	$\underline{\mathbf{e}}_{2\sigma}$	(0.000, 0.000, 1.000)	(0.000, 0.000, 1.000)
+142	$\underline{\mathbf{e}}_{3\sigma}$	(0.000, 1.000, 0.000)	(1.000, 0.000, 0.000)
+143	$\underline{\mathbf{e}}_{1\sigma}$	(0.000, 0.000, 1.000)	(0.000, 0.000, 1.000)
+143	$\underline{\mathbf{e}}_{2\sigma}$	(0.000, 1.000, 0.000)	(0.000, 1.000, 0.000)
+143	$\underline{\mathbf{e}}_{3\sigma}$	(1.000, 0.000, 0.000)	(1.000, 0.000, 0.000)
+144	$\underline{\mathbf{e}}_{1\sigma}$		(0.000, 0.000, 1.000)
+144	$\underline{\mathbf{e}}_{2\sigma}$		(0.000, 1.000, 0.000)
+144	$\underline{\mathbf{e}}_{3\sigma}$		(1.000, 0.000, 0.000)

Table S4(c). The stress tensor $\boldsymbol{\sigma}(\mathbf{r})$ eigenvectors $\{\underline{\mathbf{e}}_{1\sigma}, \underline{\mathbf{e}}_{2\sigma}, \underline{\mathbf{e}}_{3\sigma}\}$ for the $\mathbf{E}_y$-field (in a.u.) of the (Li-Li) molecules. See **Table S4(a)** for further details.

$\mathbf{E}_y$-field	Eigen-Vectors	*BCP*(Li1-*NNA*3) (*x*, *y*, *z*)	*BCP*(Li2-*NNA*3 or *NNA4*) (*x*, *y*, *z*)	*BCP*(*NNA*3- *NNA*4) (*x*, *y*, *z*)
0	$\underline{\mathbf{e}}_{1\sigma}$	(1.000, 0.000, 0.000)	(1.000, 0.000, 0.000)	
0	$\underline{\mathbf{e}}_{2\sigma}$	(0.000, 1.000, 0.000)	(0.000, 1.000, 0.000)	
0	$\underline{\mathbf{e}}_{3\sigma}$	(0.000, 0.000, 1.000)	(0.000, 0.000, 1.000)	
-20	$\underline{\mathbf{e}}_{1\sigma}$	(0.999, -0.044, 0.000)	(0.999, 0.044, 0.000)	
-20	$\underline{\mathbf{e}}_{2\sigma}$	(0.000, 0.000, 1.000)	(0.000, 0.000, 1.000)	
-20	$\underline{\mathbf{e}}_{3\sigma}$	(0.044, 0.999, 0.000)	(-0.044, 0.999, 0.000)	
-40	$\underline{\mathbf{e}}_{1\sigma}$	(0.996, -0.087, 0.000)	(0.996, 0.087, 0.000)	
-40	$\underline{\mathbf{e}}_{2\sigma}$	(0.000, 0.000, 1.000)	(0.000, 0.000, 1.000)	
-40	$\underline{\mathbf{e}}_{3\sigma}$	(0.087, 0.996, 0.000)	(-0.087, 0.996, 0.000)	
-60	$\underline{\mathbf{e}}_{1\sigma}$	(0.991, -0.131, 0.000)	(0.991, 0.131, 0.000)	
-60	$\underline{\mathbf{e}}_{2\sigma}$	(0.000, 0.000, 1.000)	(0.000, 0.000, 1.000)	
-60	$\underline{\mathbf{e}}_{3\sigma}$	(0.131, 0.991, 0.000)	(-0.131, 0.991, 0.000)	
-80	$\underline{\mathbf{e}}_{1\sigma}$	(0.985, -0.175, 0.000)	(0.985, 0.175, 0.000)	
-80	$\underline{\mathbf{e}}_{2\sigma}$	(0.000, 0.000, 1.000)	(0.000, 0.000, 1.000)	
-80	$\underline{\mathbf{e}}_{3\sigma}$	(0.175, 0.985, 0.000)	(-0.175, 0.985, 0.000)	
-100	$\underline{\mathbf{e}}_{1\sigma}$	(0.976, -0.219, 0.000)	(0.976, 0.219, 0.000)	
-100	$\underline{\mathbf{e}}_{2\sigma}$	(0.000, 0.000, 1.000)	(0.000, 0.000, 1.000)	
-100	$\underline{\mathbf{e}}_{3\sigma}$	(0.219, 0.976, 0.000)	(-0.219, 0.976, 0.000)	
-120	$\underline{\mathbf{e}}_{1\sigma}$	(0.965, -0.263, 0.000)	(0.965, 0.263, 0.000)	
-120	$\underline{\mathbf{e}}_{2\sigma}$	(0.000, 0.000, 1.000)	(0.000, 0.000, 1.000)	
-120	$\underline{\mathbf{e}}_{3\sigma}$	(0.263, 0.965, 0.000)	(-0.263, 0.965, 0.000)	
-140	$\underline{\mathbf{e}}_{1\sigma}$	(0.951, -0.308, 0.000)	(0.951, 0.308, 0.000)	
-140	$\underline{\mathbf{e}}_{2\sigma}$	(0.000, 0.000, 1.000)	(0.000, 0.000, 1.000)	

-140	$\underline{\mathbf{e}}_{3\sigma}$	(0.308, 0.951, 0.000)	(-0.308, 0.951, 0.000)	
-160	$\underline{\mathbf{e}}_{1\sigma}$	(0.935, -0.356, 0.000)	(0.935, 0.356, 0.000)	
-160	$\underline{\mathbf{e}}_{2\sigma}$	(0.000, 0.000, 1.000)	(0.000, 0.000, 1.000)	
-160	$\underline{\mathbf{e}}_{3\sigma}$	(0.356, 0.935, 0.000)	(-0.356, 0.935, 0.000)	
-180	$\underline{\mathbf{e}}_{1\sigma}$	(0.913, -0.407, 0.000)	(0.913, 0.407, 0.000)	
-180	$\underline{\mathbf{e}}_{2\sigma}$	(0.000, 0.000, 1.000)	(0.000, 0.000, 1.000)	
-180	$\underline{\mathbf{e}}_{3\sigma}$	(0.407, 0.913, 0.000)	(-0.407, 0.913, 0.000)	
-200	$\underline{\mathbf{e}}_{1\sigma}$	(0.885, -0.465, 0.000)	(0.885, 0.465, 0.000)	
-200	$\underline{\mathbf{e}}_{2\sigma}$	(0.000, 0.000, 1.000)	(0.000, 0.000, 1.000)	
-200	$\underline{\mathbf{e}}_{3\sigma}$	(0.465, 0.885, 0.000)	(-0.465, 0.885, 0.000)	
-220	$\underline{\mathbf{e}}_{1\sigma}$	(0.845, -0.534, 0.000)	(0.845, 0.534, 0.000)	
-220	$\underline{\mathbf{e}}_{2\sigma}$	(0.000, 0.000, 1.000)	(0.000, 0.000, 1.000)	
-220	$\underline{\mathbf{e}}_{3\sigma}$	(0.534, 0.845, 0.000)	(-0.534, 0.845, 0.000)	
-240	$\underline{\mathbf{e}}_{1\sigma}$	(0.787, -0.617, 0.000)	(0.787, 0.617, 0.000)	
-240	$\underline{\mathbf{e}}_{2\sigma}$	(0.000, 0.000, 1.000)	(0.000, 0.000, 1.000)	
-240	$\underline{\mathbf{e}}_{3\sigma}$	(0.617, 0.787, 0.000)	(-0.617, 0.787, 0.000)	
-255	$\underline{\mathbf{e}}_{1\sigma}$	(0.722, -0.691, 0.000)	(0.722, 0.691, 0.000)	
-255	$\underline{\mathbf{e}}_{2\sigma}$	(0.000, 0.000, 1.000)	(0.000, 0.000, 1.000)	
-255	$\underline{\mathbf{e}}_{3\sigma}$	(0.691, 0.722, 0.000)	(-0.691, 0.722, 0.000)	
-256	$\underline{\mathbf{e}}_{1\sigma}$	(0.717, -0.697, 0.000)	(0.717, 0.697, 0.000)	(0.000, 1.000, 0.000)
-256	$\underline{\mathbf{e}}_{2\sigma}$	(0.000, 0.000, 1.000)	(0.000, 0.000, 1.000)	(0.000, 0.000, 1.000)
-256	$\underline{\mathbf{e}}_{3\sigma}$	(0.697, 0.717, 0.000)	(-0.697, 0.717, 0.000)	(1.000, 0.000, 0.000)
-257	$\underline{\mathbf{e}}_{1\sigma}$	(0.711, -0.703, 0.000)	(0.711, 0.703, 0.000)	(0.000, 1.000, 0.000)
-257	$\underline{\mathbf{e}}_{2\sigma}$	(0.000, 0.000, 1.000)	(0.000, 0.000, 1.000)	(0.000, 0.000, 1.000)
-257	$\underline{\mathbf{e}}_{3\sigma}$	(0.703, 0.711, 0.000)	(-0.703, 0.711, 0.000)	(1.000, 0.000, 0.000)
-258	$\underline{\mathbf{e}}_{1\sigma}$	(-0.706, 0.709, 0.000)	(0.706, 0.709, 0.000)	(0.000, 1.000, 0.000)
-258	$\underline{\mathbf{e}}_{2\sigma}$	(0.000, 0.000, 1.000)	(0.000, 0.000, 1.000)	(0.000, 0.000, 1.000)
-258	$\underline{\mathbf{e}}_{3\sigma}$	(0.709, 0.706, 0.000)	(0.709, -0.706, 0.000)	(1.000, 0.000, 0.000)
-262	$\underline{\mathbf{e}}_{1\sigma}$	(-0.678, 0.735, 0.000)	(0.678, 0.735, 0.000)	(0.000, 1.000, 0.000)
-262	$\underline{\mathbf{e}}_{2\sigma}$	(0.000, 0.000, 1.000)	(0.000, 0.000, 1.000)	(0.000, 0.000, 1.000)
-262	$\underline{\mathbf{e}}_{3\sigma}$	(0.735, 0.678, 0.000)	(0.735, -0.678, 0.000)	(1.000, 0.000, 0.000)
-266	$\underline{\mathbf{e}}_{1\sigma}$	(-0.637, 0.771, 0.000)	(0.637, 0.771, 0.000)	(0.000, 1.000, 0.000)
-266	$\underline{\mathbf{e}}_{2\sigma}$	(0.000, 0.000, 1.000)	(0.000, 0.000, 1.000)	(0.000, 0.000, 1.000)
-266	$\underline{\mathbf{e}}_{3\sigma}$	(0.771, 0.637, 0.000)	(0.771, -0.637, 0.000)	(1.000, 0.000, 0.000)
-269	$\underline{\mathbf{e}}_{1\sigma}$	(-0.560, 0.828, 0.000)	(0.560, 0.828, 0.000)	(0.000, 1.000, 0.000)
-269	$\underline{\mathbf{e}}_{2\sigma}$	(0.000, 0.000, 1.000)	(0.000, 0.000, 1.000)	(0.000, 0.000, 1.000)
-269	$\underline{\mathbf{e}}_{3\sigma}$	(0.828, 0.560, 0.000)	(0.828, -0.560, 0.000)	(1.000, 0.000, 0.000)
-270	$\underline{\mathbf{e}}_{1\sigma}$	(0.000, 1.000, 0.000)		
-270	$\underline{\mathbf{e}}_{2\sigma}$	(0.000, 0.000, 1.000)		
-270	$\underline{\mathbf{e}}_{3\sigma}$	(1.000, 0.000, 0.000)		
-271	$\underline{\mathbf{e}}_{1\sigma}$	(0.000, 1.000, 0.000)		
-271	$\underline{\mathbf{e}}_{2\sigma}$	(0.000, 0.000, 1.000)		

-271	$\underline{\mathbf{e}}_{3\sigma}$	(1.000, 0.000, 0.000)
-274	$\underline{\mathbf{e}}_{1\sigma}$	(0.000, 1.000, 0.000)
-274	$\underline{\mathbf{e}}_{2\sigma}$	(0.000, 0.000, 1.000)
-274	$\underline{\mathbf{e}}_{3\sigma}$	(1.000, 0.000, 0.000)
-278	$\underline{\mathbf{e}}_{1\sigma}$	(0.000, 1.000, 0.000)
-278	$\underline{\mathbf{e}}_{2\sigma}$	(0.000, 0.000, 1.000)
-278	$\underline{\mathbf{e}}_{3\sigma}$	(1.000, 0.000, 0.000)
-282	$\underline{\mathbf{e}}_{1\sigma}$	(0.000, 1.000, 0.000)
-282	$\underline{\mathbf{e}}_{2\sigma}$	(0.000, 0.000, 1.000)
-282	$\underline{\mathbf{e}}_{3\sigma}$	(1.000, 0.000, 0.000)
-286	$\underline{\mathbf{e}}_{1\sigma}$	(0.000, 1.000, 0.000)
-286	$\underline{\mathbf{e}}_{2\sigma}$	(0.000, 0.000, 1.000)
-286	$\underline{\mathbf{e}}_{3\sigma}$	(1.000, 0.000, 0.000)
-294	$\underline{\mathbf{e}}_{1\sigma}$	(0.000, 1.000, 0.000)
-294	$\underline{\mathbf{e}}_{2\sigma}$	(0.000, 0.000, 1.000)
-294	$\underline{\mathbf{e}}_{3\sigma}$	(1.000, 0.000, 0.000)

Table S4(d). The stress tensor $\boldsymbol{\sigma}(\mathbf{r})$ eigenvectors $\{\underline{\mathbf{e}}_{1\sigma}, \underline{\mathbf{e}}_{2\sigma}, \underline{\mathbf{e}}_{3\sigma}\}$ for the $\mathbf{E}_y$-field (in a.u.) of the (Li-Li) molecules. See **Table S4(a)** for further details.

$\mathbf{E}_y$-field	Eigen-Vectors	*BCP*(Li1-*NNA*3) (*x*, *y*, *z*)	*BCP*(Li2-*NNA*3 or *NNA4*) (*x*, *y*, *z*)	*BCP*(*NNA*3- *NNA*4) (*x*, *y*, *z*)
0	$\underline{\mathbf{e}}_{1\sigma}$	(1.000, 0.000, 0.000)	(1.000, 0.000, 0.000)	
0	$\underline{\mathbf{e}}_{2\sigma}$	(0.000, 1.000, 0.000)	(0.000, 1.000, 0.000)	
0	$\underline{\mathbf{e}}_{3\sigma}$	(0.000, 0.000, 1.000)	(0.000, 0.000, 1.000)	
+20	$\underline{\mathbf{e}}_{1\sigma}$	(0.999, 0.044, 0.000)	(0.999, -0.044, 0.000)	
+20	$\underline{\mathbf{e}}_{2\sigma}$	(0.000, 0.000, 1.000)	(0.000, 0.000, 1.000)	
+20	$\underline{\mathbf{e}}_{3\sigma}$	(-0.044, 0.999, 0.000)	(0.044, 0.999, 0.000)	
+40	$\underline{\mathbf{e}}_{1\sigma}$	(0.996, 0.087, 0.000)	(0.996, -0.087, 0.000)	
+40	$\underline{\mathbf{e}}_{2\sigma}$	(0.000, 0.000, 1.000)	(0.000, 0.000, 1.000)	
+40	$\underline{\mathbf{e}}_{3\sigma}$	(-0.087, 0.996, 0.000)	(0.087, 0.996, 0.000)	
+60	$\underline{\mathbf{e}}_{1\sigma}$	(0.991, 0.131, 0.000)	(0.991, -0.131, 0.000)	
+60	$\underline{\mathbf{e}}_{2\sigma}$	(0.000, 0.000, 1.000)	(0.000, 0.000, 1.000)	
+60	$\underline{\mathbf{e}}_{3\sigma}$	(-0.131, 0.991, 0.000)	(0.131, 0.991, 0.000)	
+80	$\underline{\mathbf{e}}_{1\sigma}$	(0.985, 0.175, 0.000)	(0.985, -0.175, 0.000)	
+80	$\underline{\mathbf{e}}_{2\sigma}$	(0.000, 0.000, 1.000)	(0.000, 0.000, 1.000)	
+80	$\underline{\mathbf{e}}_{3\sigma}$	(-0.175, 0.985, 0.000)	(0.175, 0.985, 0.000)	
+100	$\underline{\mathbf{e}}_{1\sigma}$	(0.976, 0.219, 0.000)	(0.976, -0.219, 0.000)	
+100	$\underline{\mathbf{e}}_{2\sigma}$	(0.000, 0.000, 1.000)	(0.000, 0.000, 1.000)	
+100	$\underline{\mathbf{e}}_{3\sigma}$	(-0.219, 0.976, 0.000)	(0.219, 0.976, 0.000)	
+120	$\underline{\mathbf{e}}_{1\sigma}$	(0.965, 0.263, 0.000)	(0.965, -0.263, 0.000)	
+120	$\underline{\mathbf{e}}_{2\sigma}$	(0.000, 0.000, 1.000)	(0.000, 0.000, 1.000)	
+120	$\underline{\mathbf{e}}_{3\sigma}$	(-0.263, 0.965, 0.000)	(0.263, 0.965, 0.000)	

+140	$\underline{\mathbf{e}}_{1\sigma}$	(0.951, 0.308, 0.000)	(0.951, -0.308, 0.000)	
+140	$\underline{\mathbf{e}}_{2\sigma}$	(0.000, 0.000, 1.000)	(0.000, 0.000, 1.000)	
+140	$\underline{\mathbf{e}}_{3\sigma}$	(-0.308, 0.951, 0.000)	(0.308, 0.951, 0.000)	
+160	$\underline{\mathbf{e}}_{1\sigma}$	(0.935, 0.356, 0.000)	(0.935, -0.356, 0.000)	
+160	$\underline{\mathbf{e}}_{2\sigma}$	(0.000, 0.000, 1.000)	(0.000, 0.000, 1.000)	
+160	$\underline{\mathbf{e}}_{3\sigma}$	(-0.356, 0.935, 0.000)	(0.356, 0.935, 0.000)	
+180	$\underline{\mathbf{e}}_{1\sigma}$	(0.913, 0.407, 0.000)	(0.913, -0.407, 0.000)	
+180	$\underline{\mathbf{e}}_{2\sigma}$	(0.000, 0.000, 1.000)	(0.000, 0.000, 1.000)	
+180	$\underline{\mathbf{e}}_{3\sigma}$	(-0.407, 0.913, 0.000)	(0.407, 0.913, 0.000)	
+200	$\underline{\mathbf{e}}_{1\sigma}$	(0.885, 0.465, 0.000)	(0.885, -0.465, 0.000)	
+200	$\underline{\mathbf{e}}_{2\sigma}$	(0.000, 0.000, 1.000)	(0.000, 0.000, 1.000)	
+200	$\underline{\mathbf{e}}_{3\sigma}$	(-0.465, 0.885, 0.000)	(0.465, 0.885, 0.000)	
+220	$\underline{\mathbf{e}}_{1\sigma}$	(0.845, 0.534, 0.000)	(0.845, -0.534, 0.000)	
+220	$\underline{\mathbf{e}}_{2\sigma}$	(0.000, 0.000, 1.000)	(0.000, 0.000, 1.000)	
+220	$\underline{\mathbf{e}}_{3\sigma}$	(-0.534, 0.845, 0.000)	(0.534, 0.845, 0.000)	
+240	$\underline{\mathbf{e}}_{1\sigma}$	(0.787, 0.617, 0.000)	(0.787, -0.617, 0.000)	
+240	$\underline{\mathbf{e}}_{2\sigma}$	(0.000, 0.000, 1.000)	(0.000, 0.000, 1.000)	
+240	$\underline{\mathbf{e}}_{3\sigma}$	(-0.617, 0.787, 0.000)	(0.617, 0.787, 0.000)	
+255	$\underline{\mathbf{e}}_{1\sigma}$	(0.722, 0.691, 0.000)	(0.722, -0.691, 0.000)	
+255	$\underline{\mathbf{e}}_{2\sigma}$	(0.000, 0.000, 1.000)	(0.000, 0.000, 1.000)	
+255	$\underline{\mathbf{e}}_{3\sigma}$	(-0.691, 0.722, 0.000)	(0.691, 0.722, 0.000)	
+256	$\underline{\mathbf{e}}_{1\sigma}$	(0.717, 0.697, 0.000)	(0.717, -0.697, 0.000)	(0.000, 1.000, 0.000)
+256	$\underline{\mathbf{e}}_{2\sigma}$	(0.000, 0.000, 1.000)	(0.000, 0.000, 1.000)	(0.000, 0.000, 1.000)
+256	$\underline{\mathbf{e}}_{3\sigma}$	(-0.697, 0.717, 0.000)	(0.697, 0.717, 0.000)	(1.000, 0.000, 0.000)
+257	$\underline{\mathbf{e}}_{1\sigma}$	(0.711, 0.703, 0.000)	(0.711, -0.703, 0.000)	(0.000, 1.000, 0.000)
+257	$\underline{\mathbf{e}}_{2\sigma}$	(0.000, 0.000, 1.000)	(0.000, 0.000, 1.000)	(0.000, 0.000, 1.000)
+257	$\underline{\mathbf{e}}_{3\sigma}$	(-0.703, 0.711, 0.000)	(0.703, 0.711, 0.000)	(1.000, 0.000, 0.000)
+258	$\underline{\mathbf{e}}_{1\sigma}$	(0.706, 0.709, 0.000)	(-0.706, 0.709, 0.000)	(0.000, 1.000, 0.000)
+258	$\underline{\mathbf{e}}_{2\sigma}$	(0.000, 0.000, 1.000)	(0.000, 0.000, 1.000)	(0.000, 0.000, 1.000)
+258	$\underline{\mathbf{e}}_{3\sigma}$	(0.709, -0.706, 0.000)	(0.709, 0.706, 0.000)	(1.000, 0.000, 0.000)
+262	$\underline{\mathbf{e}}_{1\sigma}$	(0.678, 0.735, 0.000)	(-0.678, 0.735, 0.000)	(0.000, 1.000, 0.000)
+262	$\underline{\mathbf{e}}_{2\sigma}$	(0.000, 0.000, 1.000)	(0.000, 0.000, 1.000)	(0.000, 0.000, 1.000)
+262	$\underline{\mathbf{e}}_{3\sigma}$	(0.735, 0.678, 0.000)	(0.735, 0.678, 0.000)	(1.000, 0.000, 0.000)
+266	$\underline{\mathbf{e}}_{1\sigma}$	(0.637, 0.771, 0.000)	(-0.637, 0.771, 0.000)	(0.000, 1.000, 0.000)
+266	$\underline{\mathbf{e}}_{2\sigma}$	(0.000, 0.000, 1.000)	(0.000, 0.000, 1.000)	(0.000, 0.000, 1.000)
+266	$\underline{\mathbf{e}}_{3\sigma}$	(0.771, -0.637, 0.000)	(0.771, 0.637, 0.000)	(1.000, 0.000, 0.000)
+269	$\underline{\mathbf{e}}_{1\sigma}$	(0.560, 0.828, 0.000)	(-0.560, 0.828, 0.000)	(0.000, 1.000, 0.000)
+269	$\underline{\mathbf{e}}_{2\sigma}$	(0.000, 0.000, 1.000)	(0.000, 0.000, 1.000)	(0.000, 0.000, 1.000)
+269	$\underline{\mathbf{e}}_{3\sigma}$	(0.828, -0.560, 0.000)	(0.828, 0.560, 0.000)	(1.000, 0.000, 0.000)
+270	$\underline{\mathbf{e}}_{1\sigma}$	(0.000, 1.000, 0.000)		
+270	$\underline{\mathbf{e}}_{2\sigma}$	(0.000, 0.000, 1.000)		
+270	$\underline{\mathbf{e}}_{3\sigma}$	(1.000, 0.000, 0.000)		
+271	$\underline{\mathbf{e}}_{1\sigma}$	(0.000, 1.000, 0.000)		
+271	$\underline{\mathbf{e}}_{2\sigma}$	(0.000, 0.000, 1.000)		

+271	$\underline{\mathbf{e}}_{3\sigma}$	(1.000, 0.000, 0.000)
+274	$\underline{\mathbf{e}}_{1\sigma}$	(0.000, 1.000, 0.000)
+274	$\underline{\mathbf{e}}_{2\sigma}$	(0.000, 0.000, 1.000)
+274	$\underline{\mathbf{e}}_{3\sigma}$	(1.000, 0.000, 0.000)
+278	$\underline{\mathbf{e}}_{1\sigma}$	(0.000, 1.000, 0.000)
+278	$\underline{\mathbf{e}}_{2\sigma}$	(0.000, 0.000, 1.000)
+278	$\underline{\mathbf{e}}_{3\sigma}$	(1.000, 0.000, 0.000)
+282	$\underline{\mathbf{e}}_{1\sigma}$	(0.000, 1.000, 0.000)
+282	$\underline{\mathbf{e}}_{2\sigma}$	(0.000, 0.000, 1.000)
+282	$\underline{\mathbf{e}}_{3\sigma}$	(1.000, 0.000, 0.000)
+286	$\underline{\mathbf{e}}_{1\sigma}$	(0.000, 1.000, 0.000)
+286	$\underline{\mathbf{e}}_{2\sigma}$	(0.000, 0.000, 1.000)
+286	$\underline{\mathbf{e}}_{3\sigma}$	(1.000, 0.000, 0.000)
+294	$\underline{\mathbf{e}}_{1\sigma}$	(0.000, 1.000, 0.000)
+294	$\underline{\mathbf{e}}_{2\sigma}$	(0.000, 0.000, 1.000)
+294	$\underline{\mathbf{e}}_{3\sigma}$	(1.000, 0.000, 0.000)

5. Supplementary Materials S5. Hessian of $\rho(\mathbf{r})$ eigenvectors subjected to an electric field.

Table S5(a). The Hessian of $\rho(\mathbf{r})$ eigenvectors $\{\underline{\mathbf{e}}_1, \underline{\mathbf{e}}_2, \underline{\mathbf{e}}_3\}$ for the $\mathbf{E}_x$-field (in a.u.) of the (Li-Li) molecules. The *x*-axis is aligned with the bond-path in each case for all entries in **Table S5(a)-Table S5(d)**. Note, for **E**-field = -144 there is only an Li1-Li2 *BCP.* A multiplication factor of $x10^{-4}$ for the **E**-field should be used for all entries in **Supplementary Materials S4**.

$\mathbf{E}_x$-field	Eigen-Vectors	*BCP*(Li1-*NNA*3) (*x*, *y*, *z*)	*BCP*(Li2-*NNA*3) (*x*, *y*, *z*)
0	$\underline{\mathbf{e}}_1$	(0.000, 1.000, 0.000)	(0.000, 1.000, 0.000)
0	$\underline{\mathbf{e}}_2$	(0.000, 0.000, 1.000)	(0.000, 0.000, 1.000)
0	$\underline{\mathbf{e}}_3$	(1.000, 0.000, 0.000)	(1.000, 0.000, 0.000)
-20	$\underline{\mathbf{e}}_1$	(0.000, 1.000, 0.000)	(0.000, 0.000, 1.000)
-20	$\underline{\mathbf{e}}_2$	(0.000, 0.000, 1.000)	(0.000, 1.000, 0.000)
-20	$\underline{\mathbf{e}}_3$	(1.000, 0.000, 0.000)	(1.000, 0.000, 0.000)
-40	$\underline{\mathbf{e}}_1$	(0.000, 0.000, 1.000)	(0.000, 0.000, 1.000)
-40	$\underline{\mathbf{e}}_2$	(0.000, 1.000, 0.000)	(0.000, 1.000, 0.000)
-40	$\underline{\mathbf{e}}_3$	(1.000, 0.000, 0.000)	(1.000, 0.000, 0.000)
-60	$\underline{\mathbf{e}}_1$	(0.000, 0.000, 1.000)	(0.000, 1.000, 0.000)
-60	$\underline{\mathbf{e}}_2$	(0.000, 1.000, 0.000)	(0.000, 0.000, 1.000)
-60	$\underline{\mathbf{e}}_3$	(1.000, 0.000, 0.000)	(1.000, 0.000, 0.000)
-80	$\underline{\mathbf{e}}_1$	(0.000, 1.000, 0.000)	(0.000, 1.000, 0.000)
-80	$\underline{\mathbf{e}}_2$	(0.000, 0.000, 1.000)	(0.000, 0.000, 1.000)
-80	$\underline{\mathbf{e}}_3$	(1.000, 0.000, 0.000)	(1.000, 0.000, 0.000)
-100	$\underline{\mathbf{e}}_1$	(0.000, 0.000, 1.000)	(0.000, 0.000, 1.000)
-100	$\underline{\mathbf{e}}_2$	(0.000, 1.000, 0.000)	(0.000, 1.000, 0.000)
-100	$\underline{\mathbf{e}}_3$	(1.000, 0.000, 0.000)	(1.000, 0.000, 0.000)
-110	$\underline{\mathbf{e}}_1$	(0.000, 0.000, 1.000)	(0.000, 0.000, 1.000)
-110	$\underline{\mathbf{e}}_2$	(0.000, 1.000, 0.000)	(0.000, 1.000, 0.000)
-110	$\underline{\mathbf{e}}_3$	(1.000, 0.000, 0.000)	(1.000, 0.000, 0.000)
-120	$\underline{\mathbf{e}}_1$	(0.000, 0.000, 1.000)	(0.000, 0.000, 1.000)
-120	$\underline{\mathbf{e}}_2$	(0.000, 1.000, 0.000)	(0.000, 1.000, 0.000)
-120	$\underline{\mathbf{e}}_3$	(1.000, 0.000, 0.000)	(1.000, 0.000, 0.000)
-130	$\underline{\mathbf{e}}_1$	(0.000, 1.000, 0.000)	(0.000, 1.000, 0.000)
-130	$\underline{\mathbf{e}}_2$	(0.000, 0.000, 1.000)	(0.000, 0.000, 1.000)
-130	$\underline{\mathbf{e}}_3$	(1.000, 0.000, 0.000)	(1.000, 0.000, 0.000)
-140	$\underline{\mathbf{e}}_1$	(0.000, 1.000, 0.000)	(0.000, 1.000, 0.000)
-140	$\underline{\mathbf{e}}_2$	(0.000, 0.000, 1.000)	(0.000, 0.000, 1.000)
-140	$\underline{\mathbf{e}}_3$	(1.000, 0.000, 0.000)	(1.000, 0.000, 0.000)
-141	$\underline{\mathbf{e}}_1$	(0.000, 0.000, 1.000)	(0.000, 0.000, 1.000)
-141	$\underline{\mathbf{e}}_2$	(0.000, 1.000, 0.000)	(0.000, 1.000, 0.000)
-141	$\underline{\mathbf{e}}_3$	(1.000, 0.000, 0.000)	(1.000, 0.000, 0.000)
-142	$\underline{\mathbf{e}}_1$	(0.000, 0.000, 1.000)	(0.000, 0.000, 1.000)
-142	$\underline{\mathbf{e}}_2$	(0.000, 1.000, 0.000)	(0.000, 1.000, 0.000)

-142	$\underline{\mathbf{e}}_3$	(1.000, 0.000, 0.000)	(1.000, 0.000, 0.000)
-143	$\underline{\mathbf{e}}_1$	(0.000, 0.000, 1.000)	(0.000, 0.000, 1.000)
-143	$\underline{\mathbf{e}}_2$	(0.000, 1.000, 0.000)	(0.000, 1.000, 0.000)
-143	$\underline{\mathbf{e}}_3$	(1.000, 0.000, 0.000)	(1.000, 0.000, 0.000)
-144	$\underline{\mathbf{e}}_1$	(0.000, 1.000, 0.000)	
-144	$\underline{\mathbf{e}}_2$	(0.000, 0.000, 1.000)	
-144	$\underline{\mathbf{e}}_3$	(1.000, 0.000, 0.000)	

Table S5(b). The Hessian of $\rho(\mathbf{r})$ eigenvectors $\{\underline{\mathbf{e}}_1, \underline{\mathbf{e}}_2, \underline{\mathbf{e}}_3\}$ for the $\mathbf{E}_x$-field (in a.u.) of the (Li-Li) molecules. See **Table S5(a)** for further details. Note, for **E**-field = +144 there is only an Li1-Li2 *BCP*

$\mathbf{E}_x$-field	Eigen-Vectors	*BCP*(Li1-*NNA*3) (*x*, *y*, *z*)	*BCP*(Li2-*NNA*3) (*x*, *y*, *z*)
0	$\underline{\mathbf{e}}_1$	(0.000, 1.000, 0.000)	(0.000, 1.000, 0.000)
0	$\underline{\mathbf{e}}_2$	(0.000, 0.000, 1.000)	(0.000, 0.000, 1.000)
0	$\underline{\mathbf{e}}_3$	(1.000, 0.000, 0.000)	(1.000, 0.000, 0.000)
+20	$\underline{\mathbf{e}}_1$	(0.000, 0.000, 1.000)	(0.000, 0.000, 1.000)
+20	$\underline{\mathbf{e}}_2$	(0.000, 1.000, 0.000)	(0.000, 1.000, 0.000)
+20	$\underline{\mathbf{e}}_3$	(1.000, 0.000, 0.000)	(1.000, 0.000, 0.000)
+40	$\underline{\mathbf{e}}_1$	(0.000, 0.000, 1.000)	(0.000, 1.000, 0.000)
+40	$\underline{\mathbf{e}}_2$	(0.000, 1.000, 0.000)	(0.000, 0.000, 1.000)
+40	$\underline{\mathbf{e}}_3$	(1.000, 0.000, 0.000)	(1.000, 0.000, 0.000)
+60	$\underline{\mathbf{e}}_1$	(0.000, 1.000, 0.000)	(0.000, 1.000, 0.000)
+60	$\underline{\mathbf{e}}_2$	(0.000, 0.000, 1.000)	(0.000, 0.000, 1.000)
+60	$\underline{\mathbf{e}}_3$	(1.000, 0.000, 0.000)	(1.000, 0.000, 0.000)
+80	$\underline{\mathbf{e}}_1$	(0.000, 1.000, 0.000)	(0.000, 1.000, 0.000)
+80	$\underline{\mathbf{e}}_2$	(0.000, 0.000, 1.000)	(0.000, 0.000, 1.000)
+80	$\underline{\mathbf{e}}_3$	(1.000, 0.000, 0.000)	(1.000, 0.000, 0.000)
+100	$\underline{\mathbf{e}}_1$	(0.000, 1.000, 0.000)	(0.000, 1.000, 0.000)
+100	$\underline{\mathbf{e}}_2$	(0.000, 0.000, 1.000)	(0.000, 0.000, 1.000)
+100	$\underline{\mathbf{e}}_3$	(1.000, 0.000, 0.000)	(1.000, 0.000, 0.000)
+110	$\underline{\mathbf{e}}_1$	(0.000, 0.000, 1.000)	(0.000, 0.000, 1.000)
+110	$\underline{\mathbf{e}}_2$	(0.000, 1.000, 0.000)	(0.000, 1.000, 0.000)
+110	$\underline{\mathbf{e}}_3$	(1.000, 0.000, 0.000)	(1.000, 0.000, 0.000)
+120	$\underline{\mathbf{e}}_1$	(0.000, 1.000, 0.000)	(0.000, 1.000, 0.000)
+120	$\underline{\mathbf{e}}_2$	(0.000, 0.000, 1.000)	(0.000, 0.000, 1.000)
+120	$\underline{\mathbf{e}}_3$	(1.000, 0.000, 0.000)	(1.000, 0.000, 0.000)
+130	$\underline{\mathbf{e}}_1$	(0.000, 1.000, 0.000)	(0.000, 1.000, 0.000)
+130	$\underline{\mathbf{e}}_2$	(0.000, 0.000, 1.000)	(0.000, 0.000, 1.000)
+130	$\underline{\mathbf{e}}_3$	(1.000, 0.000, 0.000)	(1.000, 0.000, 0.000)
+140	$\underline{\mathbf{e}}_1$	(0.000, 1.000, 0.000)	(0.000, 1.000, 0.000)

+140	$\underline{\mathbf{e}}_2$	(0.000, 0.000, 1.000)	(0.000, 0.000, 1.000)
+140	$\underline{\mathbf{e}}_3$	(1.000, 0.000, 0.000)	(1.000, 0.000, 0.000)
+141	$\underline{\mathbf{e}}_1$	(0.000, 1.000, 0.000)	(0.000, 1.000, 0.000)
+141	$\underline{\mathbf{e}}_2$	(0.000, 0.000, 1.000)	(0.000, 0.000, 1.000)
+141	$\underline{\mathbf{e}}_3$	(1.000, 0.000, 0.000)	(1.000, 0.000, 0.000)
+142	$\underline{\mathbf{e}}_1$	(0.000, 0.000, 1.000)	(0.000, 1.000, 0.000)
+142	$\underline{\mathbf{e}}_2$	(0.000, 1.000, 0.000)	(0.000, 0.000, 1.000)
+142	$\underline{\mathbf{e}}_3$	(1.000, 0.000, 0.000)	(1.000, 0.000, 0.000)
+143	$\underline{\mathbf{e}}_1$	(0.000, 0.000, 1.000)	(0.000, 0.000, 1.000)
+143	$\underline{\mathbf{e}}_2$	(0.000, 1.000, 0.000)	(0.000, 1.000, 0.000)
+143	$\underline{\mathbf{e}}_3$	(1.000, 0.000, 0.000)	(1.000, 0.000, 0.000)
+144	$\underline{\mathbf{e}}_1$		(0.000,0.000, 1.000)
+144	$\underline{\mathbf{e}}_2$		(0.000,1.000, 0.000)
+144	$\underline{\mathbf{e}}_3$		(1.000,0.000, 0.000)

Table S5(c). The Hessian of $\rho(\mathbf{r})$ eigenvectors $\{\underline{\mathbf{e}}_1, \underline{\mathbf{e}}_2, \underline{\mathbf{e}}_3\}$ for the $\mathbf{E}_y$-field (in a.u.) of the (Li-Li) molecules. See **Table S5(a)** for further details. Note, for **E**-field = -270 to -294 and there is only an Li1-Li2 *BCP*

$\mathbf{E}_y$-field	Eigen-Vectors	*BCP*(Li1-*NNA*3) (*x*, *y*, *z*)	*BCP*(Li2-*NNA*3 or *NNA4*) (*x*, *y*, *z*)	*BCP*(*NNA*3- *NNA*4) (*x*, *y*, *z*)
0	$\underline{\mathbf{e}}_1$	(0.000, 1.000, 0.000)	(0.000, 1.000, 0.000)	
0	$\underline{\mathbf{e}}_2$	(0.000, 0.000, 1.000)	(0.000, 0.000, 1.000)	
0	$\underline{\mathbf{e}}_3$	(1.000, 0.000, 0.000)	(1.000, 0.000, 0.000)	
-20	$\underline{\mathbf{e}}_1$	(0.000, 0.000, 1.000)	(0.000, 0.000, 1.000)	
-20	$\underline{\mathbf{e}}_2$	(0.020, 1.000, 0.000)	(-0.020, 1.000, 0.000)	
-20	$\underline{\mathbf{e}}_3$	(1.000, -0.020, 0.000)	(1.000, 0.020, 0.000)	
-40	$\underline{\mathbf{e}}_1$	(0.000, 0.000, 1.000)	(0.000, 0.000, 1.000)	
-40	$\underline{\mathbf{e}}_2$	(0.041, 0.999, 0.000)	(-0.041, 0.999, 0.000)	
-40	$\underline{\mathbf{e}}_3$	(0.999, -0.041, 0.000)	(0.999, 0.041, 0.000)	
-60	$\underline{\mathbf{e}}_1$	(0.000, 0.000, 1.000)	(0.000, 0.000, 1.000)	
-60	$\underline{\mathbf{e}}_2$	(0.061, 0.998, 0.000)	(-0.061, 0.998, 0.000)	
-60	$\underline{\mathbf{e}}_3$	(0.998, -0.061, 0.000)	(0.998, 0.061, 0.000)	
-80	$\underline{\mathbf{e}}_1$	(0.000, 0.000, 1.000)	(0.000, 0.000, 1.000)	
-80	$\underline{\mathbf{e}}_2$	(0.081, 0.997, 0.000)	(-0.081, 0.997, 0.000)	
-80	$\underline{\mathbf{e}}_3$	(0.997, -0.081, 0.000)	(0.997, 0.081, 0.000)	
-100	$\underline{\mathbf{e}}_1$	(0.000, 0.000, 1.000)	(0.000, 0.000, 1.000)	
-100	$\underline{\mathbf{e}}_2$	(0.102, 0.995, 0.000)	(-0.102, 0.995, 0.000)	
-100	$\underline{\mathbf{e}}_3$	(0.995, -0.102, 0.000)	(0.995, 0.102, 0.000)	
-120	$\underline{\mathbf{e}}_1$	(0.000, 0.000, 1.000)	(0.000, 0.000, 1.000)	
-120	$\underline{\mathbf{e}}_2$	(0.122, 0.992, 0.000)	(-0.122, 0.992, 0.000)	
-120	$\underline{\mathbf{e}}_3$	(0.992, -0.122, 0.000)	(0.992, 0.122, 0.000)	
-140	$\underline{\mathbf{e}}_1$	(0.000, 0.000, 1.000)	(0.000, 0.000, 1.000)	

-140	$\underline{\mathbf{e}}_2$	(0.144, 0.990, 0.000)	(-0.144, 0.990, 0.000)	
-140	$\underline{\mathbf{e}}_3$	(0.990, -0.144, 0.000)	(0.990, 0.144, 0.000)	
-160	$\underline{\mathbf{e}}_1$	(0.000, 0.000, 1.000)	(0.000, 0.000, 1.000)	
-160	$\underline{\mathbf{e}}_2$	(0.166, 0.986, 0.000)	(-0.166, 0.986, 0.000)	
-160	$\underline{\mathbf{e}}_3$	(0.986, -0.166, 0.000)	(0.986, 0.166, 0.000)	
-180	$\underline{\mathbf{e}}_1$	(0.000, 0.000, 1.000)	(0.000, 0.000, 1.000)	
-180	$\underline{\mathbf{e}}_2$	(0.190, 0.982, 0.000)	(-0.190, 0.982, 0.000)	
-180	$\underline{\mathbf{e}}_3$	(0.982, -0.190, 0.000)	(0.982, 0.190, 0.000)	
-200	$\underline{\mathbf{e}}_1$	(0.000, 0.000, 1.000)	(0.000, 0.000, 1.000)	
-200	$\underline{\mathbf{e}}_2$	(0.215, 0.977, 0.000)	(-0.215, 0.977, 0.000)	
-200	$\underline{\mathbf{e}}_3$	(0.977, -0.215, 0.000)	(0.977, 0.215, 0.000)	
-220	$\underline{\mathbf{e}}_1$	(0.000, 0.000, 1.000)	(0.000, 0.000, 1.000)	
-220	$\underline{\mathbf{e}}_2$	(0.242, 0.970, 0.000)	(-0.242, 0.970, 0.000)	
-220	$\underline{\mathbf{e}}_3$	(0.970, -0.242, 0.000)	(0.970, 0.242, 0.000)	
-240	$\underline{\mathbf{e}}_1$	(0.000, 0.000, 1.000)	(0.000, 0.000, 1.000)	
-240	$\underline{\mathbf{e}}_2$	(0.269, 0.963, 0.000)	(-0.269, 0.963, 0.000)	
-240	$\underline{\mathbf{e}}_3$	(0.963, -0.269, 0.000)	(0.963, 0.269, 0.000)	
-255	$\underline{\mathbf{e}}_1$	(0.000, 0.000, 1.000)	(0.000, 0.000, 1.000)	
-255	$\underline{\mathbf{e}}_2$	(0.280, 0.960, 0.000)	(-0.280, 0.960, 0.000)	
-255	$\underline{\mathbf{e}}_3$	(0.960, -0.280, 0.000)	(0.960, 0.280, 0.000)	
-256	$\underline{\mathbf{e}}_1$	(0.000, 0.000, 1.000)	(0.000, 0.000, 1.000)	(0.000, 1.000, 0.000)
-256	$\underline{\mathbf{e}}_2$	(0.280, 0.960, 0.000)	(-0.280, 0.960, 0.000)	(0.000, 0.000, 1.000)
-256	$\underline{\mathbf{e}}_3$	(0.960, -0.280, 0.000)	(0.960, 0.280, 0.000)	(1.000, 0.000, 0.000)
-257	$\underline{\mathbf{e}}_1$	(0.000, 0.000, 1.000)	(0.000, 0.000, 1.000)	(0.000, 1.000, 0.000)
-257	$\underline{\mathbf{e}}_2$	(0.279, 0.960, 0.000)	(-0.279, 0.960, 0.000)	(0.000, 0.000, 1.000)
-257	$\underline{\mathbf{e}}_3$	(0.960, -0.279, 0.000)	(0.960, 0.279, 0.000)	(1.000, 0.000, 0.000)
-258	$\underline{\mathbf{e}}_1$	(0.000, 0.000, 1.000)	(0.000, 0.000, 1.000)	(0.000, 1.000, 0.000)
-258	$\underline{\mathbf{e}}_2$	(0.278, 0.961, 0.000)	(-0.278, 0.961, 0.000)	(0.000, 0.000, 1.000)
-258	$\underline{\mathbf{e}}_3$	(0.961, -0.278, 0.000)	(0.961, 0.278, 0.000)	(1.000, 0.000, 0.000)
-262	$\underline{\mathbf{e}}_1$	(0.000, 0.000, 1.000)	(0.000, 0.000, 1.000)	(0.000, 1.000, 0.000)
-262	$\underline{\mathbf{e}}_2$	(0.268, 0.963, 0.000)	(-0.268, 0.963, 0.000)	(0.000, 0.000, 1.000)
-262	$\underline{\mathbf{e}}_3$	(0.963, -0.268, 0.000)	(0.963, 0.268, 0.000)	(1.000, 0.000, 0.000)
-266	$\underline{\mathbf{e}}_1$	(0.000, 0.000, 1.000)	(0.000, 0.000, 1.000)	(0.000, 1.000, 0.000)
-266	$\underline{\mathbf{e}}_2$	(0.238, 0.971, 0.000)	(-0.238, 0.971, 0.000)	(0.000, 0.000, 1.000)
-266	$\underline{\mathbf{e}}_3$	(0.971, -0.238, 0.000)	(0.971, 0.238, 0.000)	(1.000, 0.000, 0.000)
-269	$\underline{\mathbf{e}}_1$	(0.000, 0.000, 1.000)	(0.000, 0.000, 1.000)	(0.000, 1.000, 0.000)
-269	$\underline{\mathbf{e}}_2$	(0.151, 0.989, 0.000)	(-0.151, 0.989, 0.000)	(0.000, 0.000, 1.000)
-269	$\underline{\mathbf{e}}_3$	(0.989, -0.151, 0.000)	(0.989, 0.151, 0.000)	(1.000, 0.000, 0.000)
-270	$\underline{\mathbf{e}}_1$	(0.000, 1.000, 0.000)		
-270	$\underline{\mathbf{e}}_2$	(0.000, 0.000, 1.000)		
-270	$\underline{\mathbf{e}}_3$	(1.000, 0.000, 0.000)		
-271	$\underline{\mathbf{e}}_1$	(0.000, 1.000, 0.000)		
-271	$\underline{\mathbf{e}}_2$	(0.000, 0.000,1.000)		
-271	$\underline{\mathbf{e}}_3$	(1.000, 0.000, 0.000)		

-274	$\underline{\mathbf{e}}_1$	(0.000, 1.000, 0.000)
-274	$\underline{\mathbf{e}}_2$	(0.000, 0.000, 1.000)
-274	$\underline{\mathbf{e}}_3$	(1.000, 0.000, 0.000)
-278	$\underline{\mathbf{e}}_1$	(0.000, 1.000, 0.000)
-278	$\underline{\mathbf{e}}_2$	(0.000, 0.000, 1.000)
-278	$\underline{\mathbf{e}}_3$	(1.000, 0.000, 0.000)
-282	$\underline{\mathbf{e}}_1$	(0.000, 1.000, 0.000)
-282	$\underline{\mathbf{e}}_2$	(0.000, 0.000, 1.000)
-282	$\underline{\mathbf{e}}_3$	(1.000, 0.000, 0.000)
-286	$\underline{\mathbf{e}}_1$	(0.000, 1.000, 0.000)
-286	$\underline{\mathbf{e}}_2$	(0.000, 0.000, 1.000)
-286	$\underline{\mathbf{e}}_3$	(1.000, 0.000, 0.000)
-294	$\underline{\mathbf{e}}_1$	(0.000, 1.000, 0.000)
-294	$\underline{\mathbf{e}}_2$	(0.000, 0.000, 1.000)
-294	$\underline{\mathbf{e}}_3$	(1.000, 0.000, 0.000)

Table S5(d). The Hessian of $\rho(\mathbf{r})$ eigenvectors $\{\underline{\mathbf{e}}_1, \underline{\mathbf{e}}_2, \underline{\mathbf{e}}_3\}$ for the $\mathbf{E}_y$-field (in a.u.) of the (Li-Li) molecules. See **Table S5(a)** for further details. Note, for **E**-field = +270 to +294 and there is only an Li1-Li2 *BCP*

$\mathbf{E}_y$-field	Eigen-Vectors	*BCP*(Li1-*NNA*3) (*x*, *y*, *z*)	*BCP*(Li2-*NNA*3 or *NNA4*) (*x*, *y*, *z*)	*BCP*(*NNA*3- *NNA*4) (*x*, *y*, *z*)
0	$\underline{\mathbf{e}}_1$	(0.000, 1.000, 0.000)	(0.000, 1.000, 0.000)	
0	$\underline{\mathbf{e}}_2$	(0.000, 0.000, 1.000)	(0.000, 0.000, 1.000)	
0	$\underline{\mathbf{e}}_3$	(1.000, 0.000, 0.000)	(1.000, 0.000, 0.000)	
+20	$\underline{\mathbf{e}}_1$	(0.000, 0.000, 1.000)	(0.000, 0.000, 1.000)	
+20	$\underline{\mathbf{e}}_2$	(-0.020, 1.000, 0.000)	(0.020, 1.000, 0.000)	
+20	$\underline{\mathbf{e}}_3$	(1.000, 0.020, 0.000)	(1.000, -0.020, 0.000)	
+40	$\underline{\mathbf{e}}_1$	(0.000, 0.000, 1.000)	(0.000, 0.000, 1.000)	
+40	$\underline{\mathbf{e}}_2$	(-0.041, 0.999, 0.000)	(0.041, 0.999, 0.000)	
+40	$\underline{\mathbf{e}}_3$	(0.999, 0.041, 0.000)	(0.999, -0.041, 0.000)	
+60	$\underline{\mathbf{e}}_1$	(0.000, 0.000, 1.000)	(0.000, 0.000, 1.000)	
+60	$\underline{\mathbf{e}}_2$	(-0.061, 0.998, 0.000)	(0.061, 0.998, 0.000)	
+60	$\underline{\mathbf{e}}_3$	(0.998, 0.061, 0.000)	(0.998, -0.061, 0.000)	
+80	$\underline{\mathbf{e}}_1$	(0.000, 0.000, 1.000)	(0.000, 0.000, 1.000)	
+80	$\underline{\mathbf{e}}_2$	(-0.081, 0.997, 0.000)	(0.081, 0.997, 0.000)	
+80	$\underline{\mathbf{e}}_3$	(0.997, 0.081, 0.000)	(0.997, -0.081, 0.000)	
+100	$\underline{\mathbf{e}}_1$	(0.000, 0.000, 1.000)	(0.000, 0.000, 1.000)	
+100	$\underline{\mathbf{e}}_2$	(-0.102, 0.995, 0.000)	(0.102, 0.995, 0.000)	
+100	$\underline{\mathbf{e}}_3$	(0.995, 0.102, 0.000)	(0.995, -0.102, 0.000)	
+120	$\underline{\mathbf{e}}_1$	(0.000, 0.000, 1.000)	(0.000, 0.000, 1.000)	
+120	$\underline{\mathbf{e}}_2$	(-0.122, 0.992, 0.000)	(0.122, 0.992, 0.000)	
+120	$\underline{\mathbf{e}}_3$	(0.992, 0.122, 0.000)	(0.992, -0.122, 0.000)	

+140	$\underline{\mathbf{e}}_1$	(0.000, 0.000, 1.000)	(0.000, 0.000, 1.000)	
+140	$\underline{\mathbf{e}}_2$	(-0.144, 0.990, 0.000)	(0.144, 0.990, 0.000)	
+140	$\underline{\mathbf{e}}_3$	(0.990, 0.144, 0.000)	(0.990, -0.144, 0.000)	
+160	$\underline{\mathbf{e}}_1$	(0.000, 0.000, 1.000)	(0.000, 0.000, 1.000)	
+160	$\underline{\mathbf{e}}_2$	(-0.166, 0.986, 0.000)	(0.166, 0.986, 0.000)	
+160	$\underline{\mathbf{e}}_3$	(0.986, 0.166, 0.000)	(0.986, -0.166, 0.000)	
+180	$\underline{\mathbf{e}}_1$	(0.000, 0.000, 1.000)	(0.000, 0.000, 1.000)	
+180	$\underline{\mathbf{e}}_2$	(-0.190, 0.982, 0.000)	(0.190, 0.982, 0.000)	
+180	$\underline{\mathbf{e}}_3$	(0.982, 0.190, 0.000)	(0.982, -0.190, 0.000)	
+200	$\underline{\mathbf{e}}_1$	(0.000, 0.000, 1.000)	(0.000, 0.000, 1.000)	
+200	$\underline{\mathbf{e}}_2$	(-0.215, 0.977, 0.000)	(0.215, 0.977, 0.000)	
+200	$\underline{\mathbf{e}}_3$	(0.977, 0.215, 0.000)	(0.977, -0.215, 0.000)	
+220	$\underline{\mathbf{e}}_1$	(0.000, 0.000, 1.000)	(0.000, 0.000, 1.000)	
+220	$\underline{\mathbf{e}}_2$	(-0.242, 0.970, 0.000)	(0.242, 0.970, 0.000)	
+220	$\underline{\mathbf{e}}_3$	(0.970, 0.242, 0.000)	(0.970, -0.242, 0.000)	
+240	$\underline{\mathbf{e}}_1$	(0.000, 0.000, 1.000)	(0.000, 0.000, 1.000)	
+240	$\underline{\mathbf{e}}_2$	(-0.269, 0.963, 0.000)	(0.269, 0.963, 0.000)	
+240	$\underline{\mathbf{e}}_3$	(0.963, 0.269, 0.000)	(0.963, -0.269, 0.000)	
+255	$\underline{\mathbf{e}}_1$	(0.000, 0.000, 1.000)	(0.000, 0.000, 1.000)	
+255	$\underline{\mathbf{e}}_2$	(-0.280, 0.960, 0.000)	(0.280, 0.960, 0.000)	
+255	$\underline{\mathbf{e}}_3$	(0.960, 0.280, 0.000)	(0.960, -0.280, 0.000)	
+256	$\underline{\mathbf{e}}_1$	(0.000, 0.000, 1.000)	(0.000, 0.000, 1.000)	(0.000, 1.000, 0.000)
+256	$\underline{\mathbf{e}}_2$	(-0.280, 0.960, 0.000)	(0.280, 0.960, 0.000)	(0.000, 0.000, 1.000)
+256	$\underline{\mathbf{e}}_3$	(0.960, 0.280, 0.000)	(0.960, -0.280, 0.000)	(1.000, 0.000, 0.000)
+257	$\underline{\mathbf{e}}_1$	(0.000, 0.000, 1.000)	(0.000, 0.000, 1.000)	(0.000, 1.000, 0.000)
+257	$\underline{\mathbf{e}}_2$	(-0.279, 0.960, 0.000)	(0.279, 0.960, 0.000)	(0.000, 0.000, 1.000)
+257	$\underline{\mathbf{e}}_3$	(0.960, 0.279, 0.000)	(0.960, -0.279, 0.000)	(1.000, 0.000, 0.000)
+258	$\underline{\mathbf{e}}_1$	(0.000, 0.000, 1.000)	(0.000, 0.000, 1.000)	(0.000, 1.000, 0.000)
+258	$\underline{\mathbf{e}}_2$	(-0.278, 0.961, 0.000)	(0.278, 0.961, 0.000)	(0.000, 0.000, 1.000)
+258	$\underline{\mathbf{e}}_3$	(0.961, 0.278, 0.000)	(0.961, -0.278, 0.000)	(1.000, 0.000, 0.000)
+262	$\underline{\mathbf{e}}_1$	(0.000, 0.000, 1.000)	(0.000, 0.000, 1.000)	(0.000, 1.000, 0.000)
+262	$\underline{\mathbf{e}}_2$	(-0.268, 0.963, 0.000)	(0.268, 0.963, 0.000)	(0.000, 0.000, 1.000)
+262	$\underline{\mathbf{e}}_3$	(0.963, 0.268, 0.000)	(0.963, -0.268, 0.000)	(1.000, 0.000, 0.000)
+266	$\underline{\mathbf{e}}_1$	(0.000, 0.000, 1.000)	(0.000, 0.000, 1.000)	(0.000, 1.000, 0.000)
+266	$\underline{\mathbf{e}}_2$	(-0.238, 0.971, 0.000)	(0.238, 0.971, 0.000)	(0.000, 0.000, 1.000)
+266	$\underline{\mathbf{e}}_3$	(0.971, 0.238, 0.000)	(0.971, -0.238, 0.000)	(1.000, 0.000, 0.000)
+269	$\underline{\mathbf{e}}_1$	(0.000, 0.000, 1.000)	(0.000, 0.000, 1.000)	(0.000, 1.000, 0.000)
+269	$\underline{\mathbf{e}}_2$	(-0.151, 0.989, 0.000)	(0.151, 0.989, 0.000)	(0.000, 0.000, 1.000)
+269	$\underline{\mathbf{e}}_3$	(0.989, 0.151, 0.000)	(0.989, -0.151, 0.000)	(1.000, 0.000, 0.000)
+270	$\underline{\mathbf{e}}_1$	(0.000, 1.000, 0.000)		
+270	$\underline{\mathbf{e}}_2$	(0.000, 0.000, 1.000)		
+270	$\underline{\mathbf{e}}_3$	(1.000, 0.000, 0.000)		
+271	$\underline{\mathbf{e}}_1$	(0.000, 1.000, 0.000)		
+271	$\underline{\mathbf{e}}_2$	(0.000, 0.000, 1.000)		

+271	$\underline{\mathbf{e}}_3$	(1.000, 0.000, 0.000)
+274	$\underline{\mathbf{e}}_1$	(0.000, 1.000, 0.000)
+274	$\underline{\mathbf{e}}_2$	(0.000, 0.000, 1.000)
+274	$\underline{\mathbf{e}}_3$	(1.000, 0.000, 0.000)
+278	$\underline{\mathbf{e}}_1$	(0.000, 1.000, 0.000)
+278	$\underline{\mathbf{e}}_2$	(0.000, 0.000, 1.000)
+278	$\underline{\mathbf{e}}_3$	(1.000, 0.000, 0.000)
+282	$\underline{\mathbf{e}}_1$	(0.000, 1.000, 0.000)
+282	$\underline{\mathbf{e}}_2$	(0.000, 0.000, 1.000)
+282	$\underline{\mathbf{e}}_3$	(1.000, 0.000, 0.000)
+286	$\underline{\mathbf{e}}_1$	(0.000, 1.000, 0.000)
+286	$\underline{\mathbf{e}}_2$	(0.000, 0.000, 1.000)
+286	$\underline{\mathbf{e}}_3$	(1.000, 0.000, 0.000)
+294	$\underline{\mathbf{e}}_1$	(0.000, 1.000, 0.000)
+294	$\underline{\mathbf{e}}_2$	(0.000, 0.000, 1.000)
+294	$\underline{\mathbf{e}}_3$	(1.000, 0.000, 0.000)

6. Supplementary Materials S6.

(a)

(b)

(c)

(d)

(e)

(f)

(g)

(h)

(i)

(j)

(k)

(l)

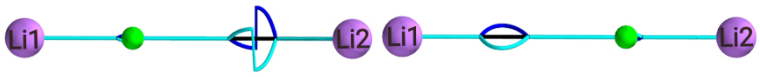

(m)

Figure S6(a). The stress tensor lithium molecular graphs displaying the $\{p_\sigma,p'_\sigma\}$ path-packets for values of the external electric field, $\mathbf{E}_x$-field (in a.u.) = $\pm 20.0\times10^{-4}$, $\pm 40.0\times10^{-4}$, $\pm 60.0\times10^{-4}$, $\pm 80.0\times10^{-4}$, $\pm 100.0\times10^{-4}$, $\pm 110.0\times10^{-4}$, $\pm 120.0\times10^{-4}$, $\pm 130.0\times10^{-4}$, $\pm 140.0\times10^{-4}$, $\pm 141.0\times10^{-4}$, $\pm 142.0\times10^{-4}$, $\pm 143.0\times10^{-4}$, $\pm 144.0\times10^{-4}$ are provided in left ($+\mathbf{E}_x$) and right ($-\mathbf{E}_x$) panels of sub-figures **(a-m)** respectively.

(a)

(b)

(c)

(d)

(e)

(f)

(g)

(h)

(i)

(j)

(k)

Figure S6(b). The stress tensor $\{p_\sigma, p'_\sigma\}$ path-packets (blue and cyan lines in right panels) for the neutral lithium Li_2 molecular graphs for values of the electric field, $\mathbf{E}_y$-field (in a.u.) = $\pm 20.0 \times 10^{-4}$, $\pm 40.0 \times 10^{-4}$, $\pm 60.0 \times 10^{-4}$, $\pm 80.0 \times 10^{-4}$, $\pm 100.0 \times 10^{-4}$, $\pm 255.0 \times 10^{-4}$, $\pm 256.0 \times 10^{-4}$, $\pm 257.0 \times 10^{-4}$, $\pm 269.0 \times 10^{-4}$, $\pm 270.0 \times 10^{-4}$ and $\pm 271.0 \times 10^{-4}$ are provided in left ($+\mathbf{E}_y$) and right ($-\mathbf{E}_y$) panels of sub-figures **(a-l)** respectively, see **Figure S6(a)** for further details.

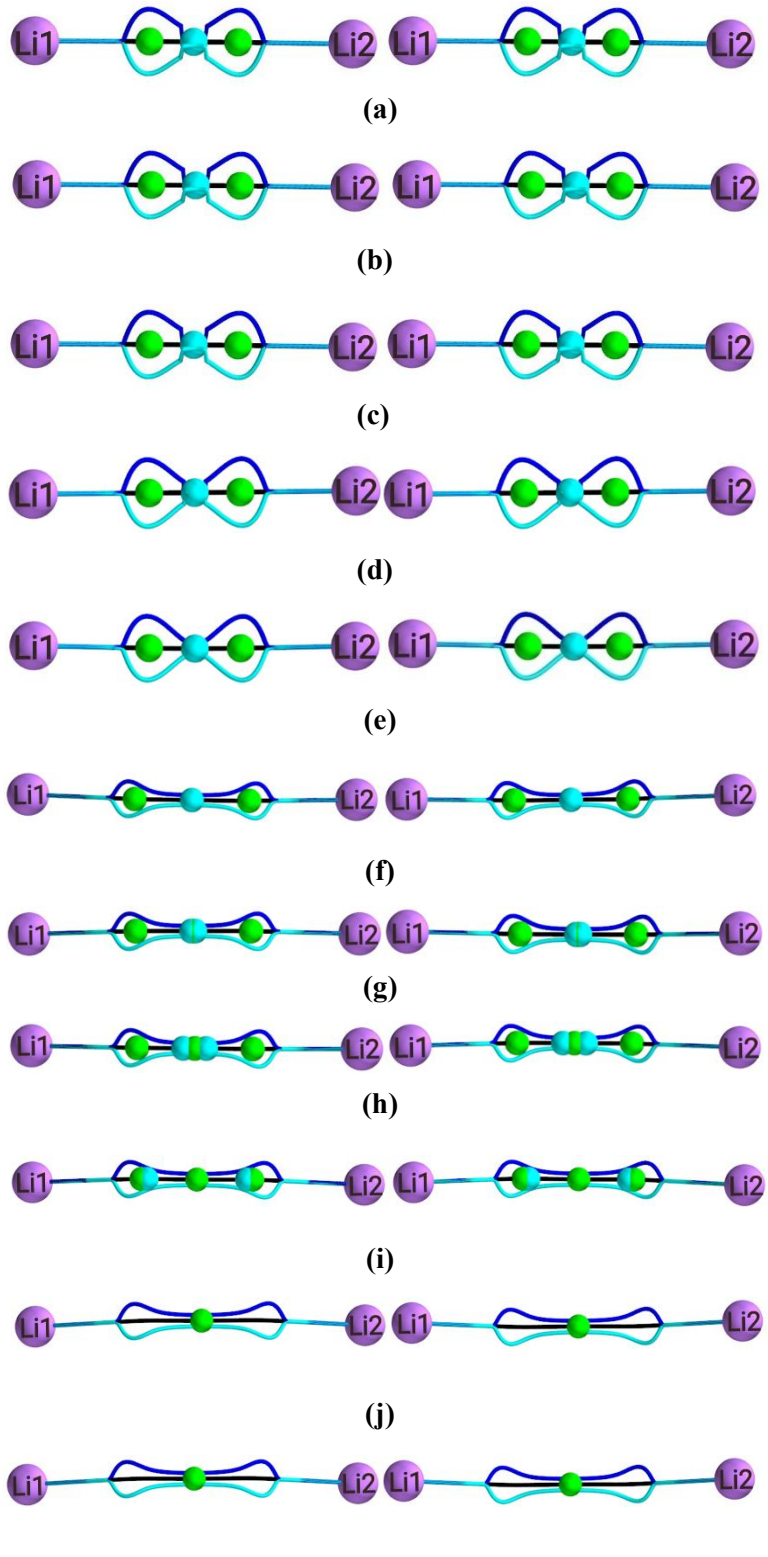

Figure S6(c). The stress tensor $\{p_\sigma, p'_\sigma\}$ path-packets (blue and cyan lines in right panels) for the neutral lithium Li_2 molecular graphs for values of the electric field, $\mathbf{E}_z$-field (in a.u.) = $\pm 20.0 \times 10^{-4}$, $\pm 40.0 \times 10^{-4}$, $\pm 60.0 \times 10^{-4}$, $\pm 80.0 \times 10^{-4}$, $\pm 100.0 \times 10^{-4}$, $\pm 255.0 \times 10^{-4}$, $\pm 256.0 \times 10^{-4}$, $\pm 257.0 \times 10^{-4}$, $\pm 269.0 \times 10^{-4}$, $\pm 270.0 \times 10^{-4}$ and $\pm 271.0 \times 10^{-4}$ are provided in left ($+\mathbf{E}_z$) and right ($-\mathbf{E}_z$) panels of sub-figures **(a-k)** respectively.

7. Supplementary Materials S7. Hessian of $\rho(\mathbf{r})$ partitioning scheme scalar QTAIM measures.

Table S8. The Hessian of $\rho(\mathbf{r})$ partitioning scheme measures for $\mathbf{E}_x$-field, $\mathbf{E}_y$-field and $\mathbf{E}_z$-field of the (Li-Li) molecules. where the bonded Li-*BCP* separations (Li–Li), Laplacian $\nabla^2\rho(\mathbf{r})$, electronic charge density $\rho(\mathbf{r})$, total local energy density $H(\mathbf{r}_b)$, metallicity $\xi(\mathbf{r}_b)$ and ellipticity ε of the *BCP* are provided, atomic units are used.

$\mathbf{E}_x$-field	*BCP*	$\rho(\mathbf{r})$	$\nabla^2\rho(\mathbf{r})$	$H(\mathbf{r}_b)$	$\xi(\mathbf{r}_b)$	ε
0	Li1-*NNA*3	0.0141	0.0028	-0.0027	4.9720	0.0000
0	Li2-*NNA*3	0.0141	0.0028	-0.0027	4.9720	0.0000
-20	Li1-*NNA*3	0.0140	0.0034	-0.0026	4.0742	0.0000
-20	Li2-*NNA*3	0.0141	0.0021	-0.0027	6.5673	0.0000
-40	Li1-*NNA*3	0.0138	0.0039	-0.0025	3.5557	0.0000
-40	Li2-*NNA*3	0.0139	0.0014	-0.0027	9.8137	0.0000
-60	Li1-*NNA*3	0.0134	0.0041	-0.0024	3.3020	0.0000
-60	Li2-*NNA*3	0.0135	0.0007	-0.0027	19.123	0.0000
-80	Li1-*NNA*3	0.0128	0.0039	-0.0023	3.3201	0.0000
-80	Li2-*NNA*3	0.0130	0.0001	-0.0026	204.64	0.0000
-100	Li1-*NNA*3	0.0121	0.0031	-0.0021	3.8557	0.0000
-100	Li2-*NNA*3	0.0121	-0.0005	-0.0024	-24.815	0.0000
-110	Li1-*NNA*3	0.0115	0.0025	-0.0020	4.6874	0.0000
-110	Li2-*NNA*3	0.0116	-0.0007	-0.0023	-15.877	0.0000
-120	Li1-*NNA*3	0.0109	0.0015	-0.0019	7.1255	0.0000
-120	Li2-*NNA*3	0.0108	-0.0010	-0.0021	-11.401	0.0000
-130	Li1-*NNA*3	0.0101	0.0002	-0.0018	44.118	0.0000
-130	Li2-*NNA*3	0.0099	-0.0012	-0.0019	-8.3932	0.0000
-140	Li1-*NNA*3	0.0088	-0.0018	-0.0016	-4.7889	0.0000

-140	Li2-*NNA*3	0.0083	-0.0015	-0.0015	-5.6664	0.0000
-141	Li1-*NNA*3	0.0086	-0.0022	-0.0016	-3.9764	0.0000
-141	Li2-*NNA*3	0.0081	-0.0015	-0.0015	-5.3536	0.0000
-142	Li1-*NNA*3	0.0084	-0.0026	-0.0015	-3.2724	0.0000
-142	Li2-*NNA*3	0.0079	-0.0016	-0.0014	-5.0147	0.0000
-143	Li1-*NNA*3	0.0081	-0.0031	-0.0015	-2.6057	0.0000
-143	Li2-*NNA*3	0.0075	-0.0016	-0.0014	-4.6301	0.0000
-144	Li1	0.0071	-0.0017	-0.0013	-4.1765	0.0000

$\mathbf{E}_x$-field	*BCP*	$\rho(\mathbf{r})$	$\nabla^2\rho(\mathbf{r})$	$H(\mathbf{r}_b)$	$\xi(\mathbf{r}_b)$	ε
0	Li1-*NNA*3	0.0141	0.0028	-0.0027	4.9720	0.0000
0	Li2-*NNA*3	0.0141	0.0028	-0.0027	4.9720	0.0000
+20	Li1-*NNA*3	0.0141	0.0021	-0.0027	6.5673	0.0000
+20	Li2-*NNA*3	0.0140	0.0034	-0.0026	4.0742	0.0000
+40	Li1-*NNA*3	0.0139	0.0014	-0.0027	9.8137	0.0000
+40	Li2-*NNA*3	0.0138	0.0039	-0.0025	3.5557	0.0000
+60	Li1-*NNA*3	0.0135	0.0007	-0.0027	19.123	0.0000
+60	Li2-*NNA*3	0.0134	0.0041	-0.0024	3.3020	0.0000
+80	Li1-*NNA*3	0.0130	0.0001	-0.0026	204.64	0.0000
+80	Li2-*NNA*3	0.0128	0.0039	-0.0023	3.3201	0.0000
+100	Li1-*NNA*3	0.0121	-0.0005	-0.0024	-24.815	0.0000
+100	Li2-*NNA*3	0.0121	0.0031	-0.0021	3.8557	0.0000
+110	Li1-*NNA*3	0.0116	-0.0007	-0.0023	-15.877	0.0000
+110	Li2-*NNA*3	0.0115	0.0025	-0.0020	4.6874	0.0000

+120	Li1-*NNA*3	0.0108	-0.0010	-0.0021	-11.401	0.0000
+120	Li2-*NNA*3	0.0109	0.0015	-0.0019	7.1255	0.0000
+130	Li1-*NNA*3	0.0099	-0.0012	-0.0019	-8.3932	0.0000
+130	Li2-*NNA*3	0.0101	0.0002	-0.0018	44.118	0.0000
+140	Li1-*NNA*3	0.0083	-0.0015	-0.0015	-5.6664	0.0000
+140	Li2-*NNA*3	0.0088	-0.0018	-0.0016	-4.7889	0.0000
+141	Li1-*NNA*3	0.0081	-0.0015	-0.0015	-5.3536	0.0000
+141	Li2-*NNA*3	0.0086	-0.0022	-0.0016	-3.9764	0.0000
+142	Li1-*NNA*3	0.0079	-0.0016	-0.0014	-5.0147	0.0000
+142	Li2-*NNA*3	0.0084	-0.0026	-0.0015	-3.2724	0.0000
+143	Li1-*NNA*3	0.0075	-0.0016	-0.0014	-4.6301	0.0000
+143	Li2-*NNA*3	0.0081	-0.0031	-0.0015	-2.6057	0.0000
+144	Li2	0.0071	-0.0017	-0.0013	-4.1765	0.0000

$\mathbf{E}_y$-field	*BCP*	$\rho(\mathbf{r})$	$\nabla^2\rho(\mathbf{r})$	$H(\mathbf{r}_b)$	$\xi(\mathbf{r}_b)$	ε
0	Li1-*NNA*3	0.0141	0.0028	-0.0027	4.9720	0.0000
0	Li2-*NNA*3	0.0141	0.0028	-0.0027	4.9720	0.0000
-20	Li1-*NNA*3	0.0141	0.0028	-0.0027	5.0405	0.0003
-20	Li2-*NNA*3	0.0141	0.0028	-0.0027	5.0405	0.0003
-40	Li1-*NNA*3	0.0140	0.0027	-0.0027	5.2589	0.0012
-40	Li2-*NNA*3	0.0140	0.0027	-0.0027	5.2589	0.0012
-60	Li1-*NNA*3	0.0139	0.0025	-0.0027	5.6722	0.0026
-60	Li2-*NNA*3	0.0139	0.0025	-0.0027	5.6722	0.0026
-80	Li1-*NNA*3	0.0137	0.0022	-0.0026	6.3833	0.0045

-80	Li2-*NNA*3	0.0137	0.0022	-0.0026	6.3833	0.0045
-100	Li1-*NNA*3	0.0135	0.0018	-0.0026	7.6305	0.0069
-100	Li2-*NNA*3	0.0135	0.0018	-0.0026	7.6305	0.0069
-120	Li1-*NNA*3	0.0132	0.0013	-0.0025	10.065	0.0096
-120	Li2-*NNA*3	0.0132	0.0013	-0.0025	10.065	0.0096
-140	Li1-*NNA*3	0.0128	0.0008	-0.0025	16.214	0.0126
-140	Li2-*NNA*3	0.0128	0.0008	-0.0025	16.214	0.0126
-160	Li1-*NNA*3	0.0123	0.0002	-0.0024	55.090	0.0161
-160	Li2-*NNA*3	0.0123	0.0002	-0.0024	55.090	0.0161
-180	Li1-*NNA*3	0.0117	-0.0004	-0.0022	-32.202	0.0204
-180	Li2-*NNA*3	0.0117	-0.0004	-0.0022	-32.202	0.0204
-200	Li1-*NNA*3	0.0109	-0.0009	-0.0021	-11.481	0.0262
-200	Li2-*NNA*3	0.0109	-0.0009	-0.0021	-11.481	0.0262
-220	Li1-*NNA*3	0.0100	-0.0015	-0.0019	-6.4712	0.0348
-220	Li2-*NNA*3	0.0100	-0.0015	-0.0019	-6.4712	0.0348
-240	Li1-*NNA*3	0.0089	-0.0022	-0.0017	-4.0331	0.0488
-240	Li2-*NNA*3	0.0089	-0.0022	-0.0017	-4.0331	0.0488
-256	Li1-*NNA*3	0.0079	-0.0029	-0.0016	-2.6698	0.0660
-256	Li2-*NNA*4	0.0079	-0.0029	-0.0016	-2.6698	0.0660
-256	*NNA*3-*NNA*4	0.0080	-0.0059	-0.0015	-1.3537	0.0994
-257	Li1-*NNA*3	0.0078	-0.0030	-0.0016	-2.5917	0.0672
-257	Li2-*NNA*3	0.0078	-0.0030	-0.0016	-2.5917	0.0672
-257	*NNA*3-*NNA*4	0.0079	-0.0058	-0.0015	-1.3591	0.1009
-258	Li1-*NNA*3	0.0077	-0.0031	-0.0015	-2.5135	0.0683
-258	Li2-*NNA*3	0.0077	-0.0031	-0.0015	-2.5135	0.0683
-258	*NNA*3-*NNA*4	0.0078	-0.0057	-0.0014	-1.3647	0.1023

-262	Li1-*NNA*3	0.0074	-0.0034	-0.0015	-2.2018	0.0719
-262	Li2-*NNA*3	0.0074	-0.0034	-0.0015	-2.2018	0.0719
-262	*NNA*3-*NNA*4	0.0075	-0.0054	-0.0014	-1.3893	0.1079
-266	Li1-*NNA*3	0.0071	-0.0038	-0.0015	-1.8744	0.0700
-266	Li2-*NNA*3	0.0071	-0.0038	-0.0015	-1.8744	0.0700
-266	*NNA*3-*NNA*4	0.0071	-0.0050	-0.0013	-1.4179	0.1131
-269	Li1-*NNA*3	0.0069	-0.0044	-0.0015	-1.5581	0.0438
-269	Li2-*NNA*3	0.0069	-0.0044	-0.0015	-1.5581	0.0438
-269	*NNA*3-*NNA*4	0.0068	-0.0047	-0.0012	-1.4434	0.1165
-270	Li1-*NNA*3	0.0067	-0.0046	-0.0012	-1.4527	0.1175
-271	Li1-*NNA*3	0.0066	-0.0045	-0.0011	-1.4625	0.1184
-274	Li1-*NNA*3	0.0063	-0.0042	-0.0011	-1.4955	0.1206
-278	Li1-*NNA*3	0.0059	-0.0038	-0.0010	-1.5512	0.1215
-282	Li1-*NNA*3	0.0054	-0.0033	-0.0008	-1.6274	0.1187
-286	Li1-*NNA*3	0.0048	-0.0027	-0.0007	-1.7430	0.1092
-294	Li1-*NNA*3	0.0030	-0.0012	-0.0003	-2.5773	0.0104
$\mathbf{E}_y$-field	*BCP*	$\rho(\mathbf{r})$	$\nabla^2\rho(\mathbf{r})$	$H(\mathbf{r}_b)$	$\xi(\mathbf{r}_b)$	ε
0	Li1-*NNA*3	0.0141	0.0028	-0.0027	4.9720	0.0000
0	Li2-*NNA*3	0.0141	0.0028	-0.0027	4.9720	0.0000
+20	Li1-*NNA*3	0.0141	0.0028	-0.0027	5.0405	0.0003
+20	Li2-*NNA*3	0.0141	0.0028	-0.0027	5.0405	0.0003
+40	Li1-*NNA*3	0.0140	0.0027	-0.0027	5.2589	0.0012
+40	Li2-*NNA*3	0.0140	0.0027	-0.0027	5.2589	0.0012
+60	Li1-*NNA*3	0.0139	0.0025	-0.0027	5.6722	0.0026
+60	Li2-*NNA*3	0.0139	0.0025	-0.0027	5.6722	0.0026

+80	Li1-*NNA*3	0.0137	0.0022	-0.0026	6.3833	0.0045
+80	Li2-*NNA*3	0.0137	0.0022	-0.0026	6.3833	0.0045
+100	Li1-*NNA*3	0.0135	0.0018	-0.0026	7.6305	0.0069
+100	Li2-*NNA*3	0.0135	0.0018	-0.0026	7.6305	0.0069
+120	Li1-*NNA*3	0.0132	0.0013	-0.0025	10.065	0.0096
+120	Li2-*NNA*3	0.0132	0.0013	-0.0025	10.065	0.0096
+140	Li1-*NNA*3	0.0128	0.0008	-0.0025	16.214	0.0126
+140	Li2-*NNA*3	0.0128	0.0008	-0.0025	16.214	0.0126
+160	Li1-*NNA*3	0.0123	0.0002	-0.0024	55.090	0.0161
+160	Li2-*NNA*3	0.0123	0.0002	-0.0024	55.090	0.0161
+180	Li1-*NNA*3	0.0117	-0.0004	-0.0022	-32.202	0.0204
+180	Li2-*NNA*3	0.0117	-0.0004	-0.0022	-32.202	0.0204
+200	Li1-*NNA*3	0.0109	-0.0009	-0.0021	-11.481	0.0262
+200	Li2-*NNA*3	0.0109	-0.0009	-0.0021	-11.481	0.0262
+220	Li1-*NNA*3	0.0100	-0.0015	-0.0019	-6.4712	0.0348
+220	Li2-*NNA*3	0.0100	-0.0015	-0.0019	-6.4712	0.0348
+240	Li1-*NNA*3	0.0089	-0.0022	-0.0017	-4.0331	0.0488
+240	Li2-*NNA*3	0.0089	-0.0022	-0.0017	-4.0331	0.0488
+256	Li1-*NNA*3	0.0079	-0.0029	-0.0016	-2.6698	0.0660
+256	Li2-*NNA*3	0.0079	-0.0029	-0.0016	-2.6698	0.0660
+256	*NNA*3-*NNA*4	0.0080	-0.0059	-0.0015	-1.3537	0.0994
+257	Li1-*NNA*3	0.0078	-0.0030	-0.0016	-2.5917	0.0672
+257	Li2-*NNA*3	0.0078	-0.0030	-0.0016	-2.5917	0.0672
+257	*NNA*3-*NNA*4	0.0079	-0.0058	-0.0015	-1.3591	0.1009
+258	Li1-*NNA*3	0.0077	-0.0031	-0.0015	-2.5135	0.0683
+258	Li2-*NNA*3	0.0077	-0.0031	-0.0015	-2.5135	0.0683

+258	*NNA*3-*NNA*4	0.0078	-0.0057	-0.0014	-1.3647	0.1023
+262	Li1-*NNA*3	0.0074	-0.0034	-0.0015	-2.2018	0.0719
+262	Li2-*NNA*3	0.0074	-0.0034	-0.0015	-2.2018	0.0719
+262	*NNA*3-*NNA*4	0.0075	-0.0054	-0.0014	-1.3893	0.1079
+266	Li1-*NNA*3	0.0071	-0.0038	-0.0015	-1.8744	0.0700
+266	Li2-*NNA*3	0.0071	-0.0038	-0.0015	-1.8744	0.0700
+266	*NNA*3-*NNA*4	0.0071	-0.0050	-0.0013	-1.4179	0.1131
+269	Li1-*NNA*3	0.0069	-0.0044	-0.0015	-1.5581	0.0438
+269	Li2-*NNA*3	0.0069	-0.0044	-0.0015	-1.5581	0.0438
+269	*NNA*3-*NNA*4	0.0068	-0.0047	-0.0012	-1.4434	0.1165
+270	Li1-*NNA*3	0.0067	-0.0046	-0.0012	-1.4527	0.1175
+271	Li1-*NNA*3	0.0066	-0.0045	-0.0011	-1.4625	0.1184
+274	Li1-*NNA*3	0.0063	-0.0042	-0.0011	-1.4955	0.1206
+278	Li1-*NNA*3	0.0059	-0.0038	-0.0010	-1.5512	0.1215
+282	Li1-*NNA*3	0.0054	-0.0033	-0.0008	-1.6274	0.1187
+286	Li1-*NNA*3	0.0048	-0.0027	-0.0007	-1.7430	0.1092
+294	Li1-*NNA*3	0.0030	-0.0012	-0.0003	-2.5773	0.0104

$\mathbf{E}_z$-field	*BCP*	$\rho(\mathbf{r})$	$\nabla^2\rho(\mathbf{r})$	$H(\mathbf{r}_b)$	$\xi(\mathbf{r}_b)$	ε
0	Li1-*NNA*3	0.0141	0.0028	-0.0027	4.9720	0.0000
0	Li2-*NNA*3	0.0141	0.0028	-0.0027	4.9720	0.0000
-20	Li1-*NNA*3	0.0141	0.0028	-0.0027	5.0405	0.0003
-20	Li2-*NNA*3	0.0141	0.0028	-0.0027	5.0405	0.0003

-40	Li1-*NNA*3	0.0140	0.0027	-0.0027	5.2589	0.0012
-40	Li2-*NNA*3	0.0140	0.0027	-0.0027	5.2589	0.0012
-60	Li1-*NNA*3	0.0139	0.0025	-0.0027	5.6722	0.0026
-60	Li2-*NNA*3	0.0139	0.0025	-0.0027	5.6722	0.0026
-80	Li1-*NNA*3	0.0137	0.0022	-0.0026	6.3833	0.0045
-80	Li2-*NNA*3	0.0137	0.0022	-0.0026	6.3833	0.0045
-100	Li1-*NNA*3	0.0135	0.0018	-0.0026	7.6305	0.0069
-100	Li2-*NNA*3	0.0135	0.0018	-0.0026	7.6305	0.0069
-120	Li1-*NNA*3	0.0132	0.0013	-0.0025	10.065	0.0096
-120	Li2-*NNA*3	0.0132	0.0013	-0.0025	10.065	0.0096
-140	Li1-*NNA*3	0.0128	0.0008	-0.0025	16.214	0.0126
-140	Li2-*NNA*3	0.0128	0.0008	-0.0025	16.214	0.0126
-160	Li1-*NNA*3	0.0123	0.0002	-0.0024	55.090	0.0161
-160	Li2-*NNA*3	0.0123	0.0002	-0.0024	55.090	0.0161
-180	Li1-*NNA*3	0.0117	-0.0004	-0.0022	-32.202	0.0204
-180	Li2-*NNA*3	0.0117	-0.0004	-0.0022	-32.202	0.0204
-200	Li1-*NNA*3	0.0109	-0.0009	-0.0021	-11.481	0.0262
-200	Li2-*NNA*3	0.0109	-0.0009	-0.0021	-11.481	0.0262
-220	Li1-*NNA*3	0.0100	-0.0015	-0.0019	-6.4712	0.0348
-220	Li2-*NNA*3	0.0100	-0.0015	-0.0019	-6.4712	0.0348
-240	Li1-*NNA*3	0.0089	-0.0022	-0.0017	-4.0331	0.0488
-240	Li2-*NNA*3	0.0089	-0.0022	-0.0017	-4.0331	0.0488
-256	Li1-*NNA*3	0.0079	-0.0029	-0.0016	-2.6698	0.0660
-256	Li2-*NNA*4	0.0079	-0.0029	-0.0016	-2.6698	0.0660
-256	*NNA*3-*NNA*4	0.0080	-0.0059	-0.0015	-1.3537	0.0994
-257	Li1-*NNA*3	0.0078	-0.0030	-0.0016	-2.5917	0.0672

-257	Li2-*NNA*3	0.0078	-0.0030	-0.0016	-2.5917	0.0672
-257	*NNA*3-*NNA*4	0.0079	-0.0058	-0.0015	-1.3591	0.1009
-258	Li1-*NNA*3	0.0077	-0.0031	-0.0015	-2.5135	0.0683
-258	Li2-*NNA*3	0.0077	-0.0031	-0.0015	-2.5135	0.0683
-258	*NNA*3-*NNA*4	0.0078	-0.0057	-0.0014	-1.3647	0.1023
-262	Li1-*NNA*3	0.0074	-0.0034	-0.0015	-2.2018	0.0719
-262	Li2-*NNA*3	0.0074	-0.0034	-0.0015	-2.2018	0.0719
-262	*NNA*3-*NNA*4	0.0075	-0.0054	-0.0014	-1.3893	0.1079
-266	Li1-*NNA*3	0.0071	-0.0038	-0.0015	-1.8744	0.0700
-266	Li2-*NNA*3	0.0071	-0.0038	-0.0015	-1.8744	0.0700
-266	*NNA*3-*NNA*4	0.0071	-0.0050	-0.0013	-1.4179	0.1131
-269	Li1-*NNA*3	0.0069	-0.0044	-0.0015	-1.5581	0.0438
-269	Li2-*NNA*3	0.0069	-0.0044	-0.0015	-1.5581	0.0438
-269	*NNA*3-*NNA*4	0.0068	-0.0047	-0.0012	-1.4434	0.1165
-270	Li1-*NNA*3	0.0067	-0.0046	-0.0012	-1.4527	0.1175
-271	Li1-*NNA*3	0.0066	-0.0045	-0.0011	-1.4625	0.1184
-274	Li1-*NNA*3	0.0063	-0.0042	-0.0011	-1.4955	0.1206
-278	Li1-*NNA*3	0.0059	-0.0038	-0.0010	-1.5512	0.1215
-282	Li1-*NNA*3	0.0054	-0.0033	-0.0008	-1.6274	0.1187
-286	Li1-*NNA*3	0.0048	-0.0027	-0.0007	-1.7430	0.1092
-294	Li1-*NNA*3	0.0030	-0.0012	-0.0003	-2.5773	0.0104

$\mathbf{E}_z$-field	*BCP*	$\rho(\mathbf{r})$	$\nabla^2\rho(\mathbf{r})$	$H(\mathbf{r}_b)$	$\xi(\mathbf{r}_b)$	ε

0	Li1-*NNA*3	0.0141	0.0028	-0.0027	4.9720	0.0000
0	Li2-*NNA*3	0.0141	0.0028	-0.0027	4.9720	0.0000
+20	Li1-*NNA*3	0.0141	0.0028	-0.0027	5.0405	0.0003
+20	Li2-*NNA*3	0.0141	0.0028	-0.0027	5.0405	0.0003
+40	Li1-*NNA*3	0.0140	0.0027	-0.0027	5.2589	0.0012
+40	Li2-*NNA*3	0.0140	0.0027	-0.0027	5.2589	0.0012
+60	Li1-*NNA*3	0.0139	0.0025	-0.0027	5.6722	0.0026
+60	Li2-*NNA*3	0.0139	0.0025	-0.0027	5.6722	0.0026
+80	Li1-*NNA*3	0.0137	0.0022	-0.0026	6.3833	0.0045
+80	Li2-*NNA*3	0.0137	0.0022	-0.0026	6.3833	0.0045
+100	Li1-*NNA*3	0.0135	0.0018	-0.0026	7.6305	0.0069
+100	Li2-*NNA*3	0.0135	0.0018	-0.0026	7.6305	0.0069
+120	Li1-*NNA*3	0.0132	0.0013	-0.0025	10.065	0.0096
+120	Li2-*NNA*3	0.0132	0.0013	-0.0025	10.065	0.0096
+140	Li1-*NNA*3	0.0128	0.0008	-0.0025	16.214	0.0126
+140	Li2-*NNA*3	0.0128	0.0008	-0.0025	16.214	0.0126
+160	Li1-*NNA*3	0.0123	0.0002	-0.0024	55.090	0.0161
+160	Li2-*NNA*3	0.0123	0.0002	-0.0024	55.090	0.0161
+180	Li1-*NNA*3	0.0117	-0.0004	-0.0022	-32.202	0.0204
+180	Li2-*NNA*3	0.0117	-0.0004	-0.0022	-32.202	0.0204
+200	Li1-*NNA*3	0.0109	-0.0009	-0.0021	-11.481	0.0262
+200	Li2-*NNA*3	0.0109	-0.0009	-0.0021	-11.481	0.0262
+220	Li1-*NNA*3	0.0100	-0.0015	-0.0019	-6.4712	0.0348
+220	Li2-*NNA*3	0.0100	-0.0015	-0.0019	-6.4712	0.0348
+240	Li1-*NNA*3	0.0089	-0.0022	-0.0017	-4.0331	0.0488
+240	Li2-*NNA*3	0.0089	-0.0022	-0.0017	-4.0331	0.0488

+256	Li1-*NNA*3	0.0079	-0.0029	-0.0016	-2.6698	0.0660
+256	Li2-*NNA*3	0.0079	-0.0029	-0.0016	-2.6698	0.0660
+256	*NNA*3-*NNA*4	0.0080	-0.0059	-0.0015	-1.3537	0.0994
+257	Li1-*NNA*3	0.0078	-0.0030	-0.0016	-2.5917	0.0672
+257	Li2-*NNA*3	0.0078	-0.0030	-0.0016	-2.5917	0.0672
+257	*NNA*3-*NNA*4	0.0079	-0.0058	-0.0015	-1.3591	0.1009
+258	Li1-*NNA*3	0.0077	-0.0031	-0.0015	-2.5135	0.0683
+258	Li2-*NNA*3	0.0077	-0.0031	-0.0015	-2.5135	0.0683
+258	*NNA*3-*NNA*4	0.0078	-0.0057	-0.0014	-1.3647	0.1023
+262	Li1-*NNA*3	0.0074	-0.0034	-0.0015	-2.2018	0.0719
+262	Li2-*NNA*3	0.0074	-0.0034	-0.0015	-2.2018	0.0719
+262	*NNA*3-*NNA*4	0.0075	-0.0054	-0.0014	-1.3893	0.1079
+266	Li1-*NNA*3	0.0071	-0.0038	-0.0015	-1.8744	0.0700
+266	Li2-*NNA*3	0.0071	-0.0038	-0.0015	-1.8744	0.0700
+266	*NNA*3-*NNA*4	0.0071	-0.0050	-0.0013	-1.4179	0.1131
+269	Li1-*NNA*3	0.0069	-0.0044	-0.0015	-1.5581	0.0438
+269	Li2-*NNA*3	0.0069	-0.0044	-0.0015	-1.5581	0.0438
+269	*NNA*3-*NNA*4	0.0068	-0.0047	-0.0012	-1.4434	0.1165
+270	Li1-*NNA*3	0.0067	-0.0046	-0.0012	-1.4527	0.1175
+271	Li1-*NNA*3	0.0066	-0.0045	-0.0011	-1.4625	0.1184
+274	Li1-*NNA*3	0.0063	-0.0042	-0.0011	-1.4955	0.1206
+278	Li1-*NNA*3	0.0059	-0.0038	-0.0010	-1.5512	0.1215
+282	Li1-*NNA*3	0.0054	-0.0033	-0.0008	-1.6274	0.1187
+286	Li1-*NNA*3	0.0048	-0.0027	-0.0007	-1.7430	0.1092
+294	Li1-*NNA*3	0.0030	-0.0012	-0.0003	-2.5773	0.0104

8. Supplementary Materials S8. Critical point separations for neutral Li_2 subjected to an electric field.

Table S8(a). Effect of the ±**E**$_x$ field on critical point (*NCP*, *NNA*, *BCP*) separations, the GBL is defined as shortest separation between nuclei, and ΔGBL1 corresponds to the distance between Li1 atom and nuclei, ΔGBL2 corresponds to the separation between Li2 atom and nuclei. The values of the inter-nuclear separations are referred to as the difference of bond-path lengths (ΔBPL) (in a.u.), where ΔBPL1(Li1-*NNA*3 *BCP*1), ΔBPL2(Li2-*NNA*3 *BCP*2). Δ(Li1-*NNA*3) and Δ(Li2-*NNA*3) correspond to the spatial straight-line separations of Li1 and *NNA*3, and Li2 and *NNA*3, respectively.

E$_x$-field	GBL1	GBL2	BPL1	BPL2	(Li1-*NNA*3)	(Li2-*NNA*3)	(Li1-*BCP*,*NNA*3-*BCP*)	(Li2-*BCP*,*NNA*3-*BCP*)
0	2.5301	2.5301	2.5301	2.5301	2.5301	2.5301	(1.8241,0.7060)	(1.8241,0.7060)
delta								
E$_x$-field	ΔGBL1	ΔGBL2	ΔBPL1	ΔBPL2	Δ(Li1-*NNA*3)	Δ(Li2-*NNA*3)	Δ(Li1-*BCP*,*NNA*3-*BCP*)	Δ(Li2-*BCP*,*NNA*3-*BCP*)
-100	0.1313	0.1479	0.1313	0.1479	0.1313	0.1479	(0.0362, 0.0951)	(0.0796, 0.0683)
-80	0.0865	0.0717	0.0865	0.0717	0.0865	0.0717	(0.0131, 0.0734)	(0.0527, 0.0189)
-60	0.0531	0.0293	0.0531	0.0293	0.0531	0.0293	(0.0013, 0.0518)	(0.0332,-0.0039)
-40	0.0280	0.0069	0.0280	0.0069	0.0280	0.0069	(-0.0038,0.0317)	(0.0184,-0.0116)
-20	0.0102	-0.0018	0.0102	-0.0018	0.0102	-0.0018	(-0.0039,0.0141)	(0.0075,-0.0093)
+20	-0.0018	0.0102	-0.0018	0.0102	-0.0018	0.0102	(0.0075,-0.0093)	(-0.0039,0.0141)
+40	0.0069	0.0280	0.0069	0.0280	0.0069	0.0280	(0.0184,-0.0116)	(-0.0038,0.0317)
+60	0.0293	0.0531	0.0293	0.0531	0.0293	0.0531	(0.0332,-0.0039)	(0.0013, 0.0518)
+80	0.0717	0.0865	0.0717	0.0865	0.0717	0.0865	(0.0527, 0.0189)	(0.0131, 0.0734)
+100	-0.0018	0.0102	0.1479	0.1313	-0.0018	0.0102	(0.0796, 0.0683)	(0.0362, 0.0951)

Table S8(b). Effect of the ±**E**-field on relative critical point separations, see the caption of **Table S8(a)** further details.

$\mathbf{E}_y$-field	GBL1	GBL2	BPL1	BPL2	(Li1-*NNA*3)	(Li2-*NNA*3)	(Li1-*BCP*, *NNA*3-*BCP*)	(Li2-*BCP*, *NNA*3-*BCP*)
0	2.5301	2.5301	2.5301	2.5301	2.5301	2.5301	(1.8241,0.7060)	(1.8241,0.7060)
$\mathbf{E}_y$-field	ΔGBL1	ΔGBL2	ΔBPL1	ΔBPL2	Δ(Li1-*NNA*3)	Δ(Li2-*NNA*3)	Δ(Li1-*BCP*, *NNA*3-*BCP*)	Δ(Li2-*BCP*, *NNA*3-*BCP*)
-200	0.2664	0.2664	0.2787	0.2787	0.2664	0.2664	(0.0009,0.0009)	(0.0009,0.0009)
-100	0.0475	0.0475	0.0496	0.0496	0.0475	0.0475	(0.0034,0.0038)	(0.0034,0.0038)
-80	0.0293	0.0293	0.0305	0.0305	0.0293	0.0293	(0.0078,0.0088)	(0.0078,0.0088)
-60	0.0160	0.0160	0.0167	0.0167	0.0160	0.0160	(0.0143,0.0518)	(0.0143,0.0518)
-40	0.0069	0.0069	0.0073	0.0073	0.0069	0.0069	(0.0232,0.0264)	(0.0232,0.0264)
-20	0.0017	0.0017	0.0018	0.0018	0.0017	0.0017	(0.1245,0.1541)	(0.1245,0.1541)
+20	0.0017	0.0017	0.0018	0.0018	0.0017	0.0017	(0.1245,0.1541)	(0.1245,0.1541)
+40	0.0069	0.0069	0.0073	0.0073	0.0069	0.0069	(0.0232,0.0264)	(0.0232,0.0264)
+60	0.0160	0.0160	0.0167	0.0167	0.0160	0.0160	(0.0143,0.0518)	(0.0143,0.0518)
+80	0.0293	0.0293	0.0305	0.0305	0.0293	0.0293	(0.0078,0.0088)	(0.0078,0.0088)
+100	0.0475	0.0475	0.0496	0.0496	0.0475	0.0475	(0.0034,0.0038)	(0.0034,0.0038)
+200	0.2664	0.2664	0.2787	0.2787	0.2664	0.2664	(0.0009,0.0009)	(0.0009,0.0009)

Table S8(c). Effect of the ±**E**-field on critical point separations, see the caption of **Table S8(a)** further details.

$\mathbf{E}_x$-field	GBL(Li1-Li2)	BPL1	BPL2	(Li1-*NNA*3)	(Li2-*NNA*3)	(Li1-*BCP*, *NNA*3-*BCP*)	(Li2-*BCP*, *NNA*3-*BCP*)
0	5.0602	2.5301	2.5301	2.5301	2.5301	(1.8241, 0.7060)	(1.8241, 0.7060)
-20	5.0686	2.5403	2.5283	2.5403	2.5283	(1.8202, 0.7201)	(1.8316, 0.6967)
+20	5.0686	2.5283	2.5403	2.5283	2.5403	(1.8316, 0.6967)	(1.8202, 0.7201)
-40	5.0951	2.5581	2.5370	2.5581	2.5370	(1.8203, 0.7377)	(1.8425, 0.6944)
+40	5.0951	2.5370	2.5581	2.5370	2.5581	(1.8425, 0.6944)	(1.8203, 0.7377)
-60	5.1426	2.5832	2.5594	2.5832	2.5594	(1.8254, 0.7578)	(1.8573, 0.7021)
+60	5.1426	2.5594	2.5832	2.5594	2.5832	(1.8573, 0.7021)	(1.8254, 0.7578)
-80	5.2184	2.6166	2.6018	2.6166	2.6018	(1.8372, 0.7794)	(1.8768, 0.7249)
+80	5.2184	2.6018	2.6166	2.6018	2.6166	(1.8768, 0.7249)	(1.8372, 0.7794)
-100	5.3394	2.6614	2.6780	2.6614	2.6780	(1.8603, 0.8011)	(1.9037, 0.7743)
+100	5.3394	2.5283	2.5403	2.6780	2.6614	(1.9037, 0.7743)	(1.8603, 0.8011)
-110	5.4286	2.6891	2.7396	2.6891	2.7396	(1.8794, 0.8097)	(1.9217, 0.8178)
+110	5.4286	2.7396	2.6891	2.7396	2.6891	(1.9217, 0.8178)	(1.8794, 0.8097)
-120	5.5513	2.7187	2.8327	2.7187	2.8327	(1.9075, 0.8112)	(1.9454, 0.8873)
+120	5.5513	2.8327	2.7187	2.8327	2.7187	(1.9454, 0.8873)	(1.9075, 0.8112)
-130	5.7339	2.7369	2.9971	2.7369	2.9971	(1.9531, 0.7838)	(2.0439, 1.3891)
+130	5.7339	2.9971	2.7369	2.9971	2.7369	(2.0439, 1.3891)	(1.9531, 0.7838)
-140	6.0704	2.6374	3.4330	2.6374	3.4330	(2.0558, 0.5816)	(2.0439, 1.3891)
+140	6.0704	3.4330	2.6374	3.4330	2.6374	(2.0439, 1.3891)	(2.0558, 0.5816)
-141	6.1272	2.5994	3.5277	2.5994	3.5277	(2.0779, 0.5216)	(2.0552, 1.4726)
+141	6.1272	3.5277	2.5994	3.5277	2.5994	(2.0552, 1.4726)	(2.0779, 0.5216)

-142	6.1949	2.5461	3.6488	2.5461	3.6488	(2.1080, 0.4381)	(2.0688, 1.5799)
+142	6.1949	3.6488	2.5461	3.6488	2.5461	(2.0688, 1.5799)	(2.1080, 0.4381)
-143	6.2806	2.4631	3.8175	2.4631	3.8175	(2.1575, 0.3056)	(2.0865, 1.7311)
+143	6.2806	3.8175	2.4631	3.8175	2.4631	(2.0865, 1.7311)	(2.1575, 0.3056)
-144	6.4062	-----	-----	-----	-----	(----- , -----)	(----- , -----)
+144	6.4062	-----	-----	-----	-----	(4.2930 , -----)	(2.1132 , -----)

E$_y$-field	GBL(Li1-Li2)	BPL1	BPL2	(Li1-*NNA*3)	(Li2-*NNA*3)	(Li1-*BCP*, *NNA*3-*BCP*)	(Li2-*BCP*, *NNA*3-*BCP*)
0	5.0602	2.5301	2.5301	2.5301	2.5301	(1.8241, 0.7060)	(1.8241, 0.7060)
-20	5.0636	2.5319	2.5319	2.5319	2.5319	(1.8250, 0.7069)	(1.8250, 0.7069)
+20	5.0636	2.5319	2.5319	2.5319	2.5319	(1.8250, 0.7069)	(1.8250, 0.7069)
-40	5.0741	2.5371	2.5374	2.5370	2.5370	(1.8275, 0.7098)	(1.8275, 0.7098)
+40	5.0741	2.5371	2.5374	2.5370	2.5370	(1.8275, 0.7098)	(1.8275, 0.7098)
-60	5.0921	2.5468	2.5468	2.5461	2.5461	(1.8319, 0.7148)	(1.8319, 0.7148)
+60	5.0921	2.5468	2.5468	2.5461	2.5461	(1.8319, 0.7148)	(1.8319, 0.7148)
-80	5.1187	2.5606	2.5606	2.5606	2.5606	(1.8384, 0.7222)	(1.8384, 0.7222)
+80	5.1187	2.5606	2.5606	2.5606	2.5606	(1.8384, 0.7222)	(1.8384, 0.7222)
-100	5.1553	2.5797	2.5797	2.5776	2.5776	(1.8473, 0.7324)	(1.8473, 0.7324)
+100	5.1553	2.5797	2.5797	2.5776	2.5776	(1.8473, 0.7324)	(1.8473, 0.7324)
-120	5.2041	2.6050	2.6050	2.6050	2.6050	(1.8590, 0.7460)	(1.8590, 0.7460)
+120	5.2041	2.6050	2.6050	2.6050	2.6050	(1.8590, 0.7460)	(1.8590, 0.7460)
-140	5.2680	2.6383	2.6383	2.6383	2.6383	(1.8741, 0.7641)	(1.8741, 0.7641)
+140	5.2680	2.6383	2.6383	2.6383	2.6383	(1.8741, 0.7641)	(1.8741, 0.7641)
-160	5.3508	2.6814	2.6814	2.6814	2.6814	(1.8934, 0.7879)	(1.8934, 0.7879)

+160	5.3508	2.6814	2.6814	2.6814	2.6814	(1.8934, 0.7879)	(1.8934, 0.7879)
-180	5.4572	2.7370	2.7370	2.7370	2.7370	(1.9178, 0.8192)	(1.9178, 0.8192)
+180	5.4572	2.7370	2.7370	2.7370	2.7370	(1.9178, 0.8192)	(1.9178, 0.8192)
-200	5.5931	2.8088	2.8088	2.8088	2.8088	(1.9486, 0.8601)	(1.9486, 0.8601)
+200	5.5931	2.8088	2.8088	2.8088	2.8088	(1.9486, 0.8601)	(1.9486, 0.8601)
-220	5.7681	2.9030	2.9030	2.9030	2.9030	(1.9888, 0.9142)	(1.9888, 0.9142)
+220	5.7681	2.9030	2.9030	2.9030	2.9030	(1.9888, 0.9142)	(1.9888, 0.9142)
-240	5.9996	3.0313	3.0313	3.0313	3.0313	(2.0452, 0.9861)	(2.0452, 0.9861)
+240	5.9996	3.0313	3.0313	3.0313	3.0313	(2.0452, 0.9861)	(2.0452, 0.9861)

$\mathbf{E_z}$-field	GBL(Li1-Li2)	BPL1	BPL2	(Li1-*NNA*3)	(Li2-*NNA*3)	(Li1-*BCP*, *NNA*3-*BCP*)	(Li2-*BCP*, *NNA*3-*BCP*)
0	5.0602	2.5301	2.5301	2.5301	2.5301	(1.8241, 0.7060)	(1.8241, 0.7060)
-20	5.0636	2.5319	2.5319	2.5319	2.5319	(1.8250, 0.7069)	(1.8250, 0.7069)
+20	5.0636	2.5319	2.5319	2.5319	2.5319	(1.8250, 0.7069)	(1.8250, 0.7069)
-40	5.0741	2.5371	2.5374	2.5370	2.5370	(1.8275, 0.7098)	(1.8275, 0.7098)
+40	5.0741	2.5371	2.5374	2.5370	2.5370	(1.8275, 0.7098)	(1.8275, 0.7098)
-60	5.0921	2.5468	2.5468	2.5461	2.5461	(1.8319, 0.7148)	(1.8319, 0.7148)
+60	5.0921	2.5468	2.5468	2.5461	2.5461	(1.8319, 0.7148)	(1.8319, 0.7148)
-80	5.1187	2.5606	2.5606	2.5606	2.5606	(1.8384, 0.7222)	(1.8384, 0.7222)
+80	5.1187	2.5606	2.5606	2.5606	2.5606	(1.8384, 0.7222)	(1.8384, 0.7222)
-100	5.1553	2.5797	2.5797	2.5776	2.5776	(1.8473, 0.7324)	(1.8473, 0.7324)
+100	5.1553	2.5797	2.5797	2.5776	2.5776	(1.8473, 0.7324)	(1.8473, 0.7324)
-120	5.2041	2.6050	2.6050	2.6050	2.6050	(1.8590, 0.7460)	(1.8590, 0.7460)
+120	5.2041	2.6050	2.6050	2.6050	2.6050	(1.8590, 0.7460)	(1.8590, 0.7460)

-140	5.2680	2.6383	2.6383	2.6383	2.6383	(1.8741, 0.7641)	(1.8741, 0.7641)
+140	5.2680	2.6383	2.6383	2.6383	2.6383	(1.8741, 0.7641)	(1.8741, 0.7641)
-160	5.3508	2.6814	2.6814	2.6814	2.6814	(1.8934, 0.7879)	(1.8934, 0.7879)
+160	5.3508	2.6814	2.6814	2.6814	2.6814	(1.8934, 0.7879)	(1.8934, 0.7879)
-180	5.4572	2.7370	2.7370	2.7370	2.7370	(1.9178, 0.8192)	(1.9178, 0.8192)
+180	5.4572	2.7370	2.7370	2.7370	2.7370	(1.9178, 0.8192)	(1.9178, 0.8192)
-200	5.5931	2.8088	2.8088	2.8088	2.8088	(1.9486, 0.8601)	(1.9486, 0.8601)
+200	5.5931	2.8088	2.8088	2.8088	2.8088	(1.9486, 0.8601)	(1.9486, 0.8601)
-220	5.7681	2.9030	2.9030	2.9030	2.9030	(1.9888, 0.9142)	(1.9888, 0.9142)
+220	5.7681	2.9030	2.9030	2.9030	2.9030	(1.9888, 0.9142)	(1.9888, 0.9142)
-240	5.9996	3.0313	3.0313	3.0313	3.0313	(2.0452, 0.9861)	(2.0452, 0.9861)
+240	5.9996	3.0313	3.0313	3.0313	3.0313	(2.0452, 0.9861)	(2.0452, 0.9861)

Table S8(d). Relative critical point separations for ±**E**-field, see the caption of **Table S8(a)** further details.

$\mathbf{E}_y$-field	(Li1-*BCP*1, *NNA*3-*BCP*1)	(Li2-*BCP*2, *NNA*4-*BCP*2)	(*NNA*3-*BCP*3, *NNA*4-*BCP*3)
-255	(2.1121, 1.0531)	(2.1121, 1.0531)	(----- , -----)
+255	(2.1121, 1.0531)	(2.1121, 1.0531)	(----- , -----)
-256	(2.1181, 1.0226)	(2.1181, 1.0226)	(3.1338, 3.1337)
+256	(2.1181, 1.0226)	(2.1181, 1.0226)	(3.1338, 3.1337)
+257	(2.1245, 0.8522)	(2.1245, 0.8522)	(0.0200, 0.0200)
-257	(2.1245, 0.8522)	(2.1245, 0.8522)	(0.0200, 0.0200)
-269	(2.2916,0.1049)	(2.2916,0.1049)	(0.9474 ,0.9474)
+269	(2.2916,0.1049)	(2.2916,0.1049)	(0.9474 ,0.9474)
-270	(3.3598, -----)	(----- , -----)	(----- , -----)
+270	(3.3598, -----)	(----- , -----)	(----- , -----)
-271	(3.3762, -----)	(----- , -----)	(----- , -----)
+271	(3.2762, -----)	(----- , -----)	(----- , -----)

$\mathbf{E}_z$-field	(Li1-*BCP*1, *NNA*3-*BCP*1)	(Li2-*BCP*2, *NNA*4-*BCP*2)	(*NNA*3-*BCP*3, *NNA*4-*BCP*3)
-255	(2.1121, 1.0531)	(2.1121, 1.0531)	(----- , -----)
+255	(2.1121, 1.0531)	(2.1121, 1.0531)	(----- , -----)
-256	(2.1181, 1.0226)	(2.1181, 1.0226)	(3.1338, 3.1337)
+256	(2.1181, 1.0226)	(2.1181, 1.0226)	(3.1338, 3.1337)
+257	(2.1245, 0.8522)	(2.1245, 0.8522)	(0.0200, 0.0200)
-257	(2.1245, 0.8522)	(2.1245, 0.8522)	(0.0200, 0.0200)
-269	(2.2916,0.1049)	(2.2916,0.1049)	(0.9474 ,0.9474)
+269	(2.2916,0.1049)	(2.2916,0.1049)	(0.9474 ,0.9474)
-270	(3.3598, -----)	(----- , -----)	(----- , -----)
+270	(3.3598, -----)	(----- , -----)	(----- , -----)
-271	(3.3762, -----)	(----- , -----)	(----- , -----)
+271	(3.2762, -----)	(----- , -----)	(----- , -----)

9. Supplementary Materials S9. Stretched neutral Li_2 for the Hessian of $\rho(\mathbf{r})$ and stress tensor $\boldsymbol{\sigma}(\mathbf{r})$.

Table S9(a). Variation of the total electronic charge density $\rho(\mathbf{r_b})$, Laplacian $\nabla^2\rho(\mathbf{r_b})$ and metallicity $\xi(\mathbf{r_b})$ of the Li1-Li2 *BCP* corresponding to the neutral Li_2 stretching distortions GBL from our previously published work[14], however the $\rho(\mathbf{r_b})$, $\nabla^2\rho(\mathbf{r_b})$ and $\xi(\mathbf{r_b})$ were only previously published for the relaxed geometry, that is displayed in an italic font, atomic units are used.

	GBL(Li1-Li2)	$\rho(\mathbf{r_b})$	$\nabla^2\rho(\mathbf{r_b})$	$\xi(\mathbf{r_b})$
(***a***)	***5.1036***	0.0135	0.0039	3.4523
(b)	6.1036	0.0096	0.0002	40.068
(c)	7.1036	0.0068	-0.0030	-2.2921
(d)	8.1036	0.0045	-0.0012	-3.6450
(e)	9.1036	0.0030	-0.0005	-6.2901
(f)	10.103	0.0020	-0.0002	-13.146
(g)	11.103	0.0013	0.0000	-87.316
(h)	12.103	0.0008	0.0000	22.301

Table S9(b). The Hessian of $\rho(\mathbf{r})$ eigenvectors $\{\underline{\mathbf{e}}_1, \underline{\mathbf{e}}_2, \underline{\mathbf{e}}_3\}$ and the stress tensor $\boldsymbol{\sigma}(\mathbf{r})$ eigenvectors $\{\underline{\mathbf{e}}_{1\sigma}, \underline{\mathbf{e}}_{2\sigma}, \underline{\mathbf{e}}_{3\sigma}\}$, for the stretching distortions of neutral Li_2 (in a.u.) of the (Li-Li) molecules provided in **Table S9(a)**. The *z*-axis is aligned with the bond-path in each case.

E-field	Eigen-Vectors	*BCP*(Li1-*NNA*3) (*x*, *y*, *z*)	*BCP*(Li2-*NNA*3) (*x*, *y*, *z*)
(***a***)			
	$\underline{\mathbf{e}}_1$	(0.000, 1.000, 0.000)	(1.000, 0.000, 0.000)
	$\underline{\mathbf{e}}_2$	(1.000, 0.000, 0.000)	(0.000, 1.000, 0.000)
	$\underline{\mathbf{e}}_3$	(0.000, 0.000, 1.000)	(0.000, 0.000, 1.000)
(b)			
	$\underline{\mathbf{e}}_1$	(0.000, 1.000, 0.000)	(1.000, 0.000, 0.000)
	$\underline{\mathbf{e}}_2$	(1.000, 0.000, 0.000)	(0.000, 1.000, 0.000)
	$\underline{\mathbf{e}}_3$	(0.000, 0.000, 1.000)	(0.000, 0.000, 1.000)
(c)			
	$\underline{\mathbf{e}}_1$	(1.000, 0.000, 0.000)	
	$\underline{\mathbf{e}}_2$	(0.000, 1.000, 0.000)	
	$\underline{\mathbf{e}}_3$	(0.000, 0.000, 1.000)	
(d)			
	$\underline{\mathbf{e}}_1$	(1.000, 0.000, 0.000)	
	$\underline{\mathbf{e}}_2$	(0.000, 1.000, 0.000)	
	$\underline{\mathbf{e}}_3$	(0.000, 0.000, 1.000)	
(e)			
	$\underline{\mathbf{e}}_1$	(1.000, 0.000, 0.000)	
	$\underline{\mathbf{e}}_2$	(0.000, 1.000, 0.000)	
	$\underline{\mathbf{e}}_3$	(0.000, 0.000, 1.000)	

(f)

$\underline{\mathbf{e}}_1$	(1.000, 0.000, 0.000)
$\underline{\mathbf{e}}_2$	(0.000, 1.000, 0.000)
$\underline{\mathbf{e}}_3$	(0.000, 0.000, 1.000)

(g)

$\underline{\mathbf{e}}_1$	(1.000, 0.000, 0.000)
$\underline{\mathbf{e}}_2$	(0.000, 1.000, 0.000)
$\underline{\mathbf{e}}_3$	(0.000, 0.000, 1.000)

(h)

$\underline{\mathbf{e}}_1$	(1.000, 0.000, 0.000)
$\underline{\mathbf{e}}_2$	(0.000, 1.000, 0.000)
$\underline{\mathbf{e}}_3$	(0.000, 0.000, 1.000)

Table S9(c). The stress tensor $\boldsymbol{\sigma}(\mathbf{r})$ eigenvectors $\{\underline{\mathbf{e}}_{1\sigma}, \underline{\mathbf{e}}_{2\sigma}, \underline{\mathbf{e}}_{3\sigma}\}$ for the stretching distortions of neutral Li_2 (in a.u.) of the (Li-Li) molecules are provided in **Table S9(a)**. The *z*-axis is aligned with the bond-path in each case.

E-field	Eigen-Vectors	*BCP*(Li1-*NNA*3) (*x*, *y*, *z*)	*BCP*(Li2-*NNA*3) (*x*, *y*, *z*)
(a)			
	$\underline{\mathbf{e}}_{1\sigma}$	(0.000, 0.000, 1.000)	(0.000, 0.000, 1.000)
	$\underline{\mathbf{e}}_{2\sigma}$	(0.000, 1.000, 0.000)	(1.000, 0.000, 0.000)
	$\underline{\mathbf{e}}_{3\sigma}$	(1.000, 0.000, 0.000)	(0.000, 1.000, 0.000)
(b)			
	$\underline{\mathbf{e}}_{1\sigma}$	(0.000, 0.000, 1.000)	(0.000, 0.000, 1.000)
	$\underline{\mathbf{e}}_{2\sigma}$	(0.000, 1.000, 0.000)	(1.000, 0.000, 0.000)
	$\underline{\mathbf{e}}_{3\sigma}$	(1.000, 0.000, 0.000)	(0.000, 1.000, 0.000)
(c)			
	$\underline{\mathbf{e}}_{1\sigma}$	(1.000, 0.000, 0.000)	
	$\underline{\mathbf{e}}_{2\sigma}$	(0.000, 1.000, 0.000)	
	$\underline{\mathbf{e}}_{3\sigma}$	(0.000, 0.000, 1.000)	
(d)			
	$\underline{\mathbf{e}}_{1\sigma}$	(1.000, 0.000, 0.000)	
	$\underline{\mathbf{e}}_{2\sigma}$	(0.000, 1.000, 0.000)	
	$\underline{\mathbf{e}}_{3\sigma}$	(0.000, 0.000, 1.000)	
(e)			
	$\underline{\mathbf{e}}_{1\sigma}$	(1.000, 0.000, 0.000)	
	$\underline{\mathbf{e}}_{2\sigma}$	(0.000, 1.000, 0.000)	
	$\underline{\mathbf{e}}_{3\sigma}$	(0.000, 0.000, 1.000)	
(f)			
	$\underline{\mathbf{e}}_{1\sigma}$	(1.000, 0.000, 0.000)	
	$\underline{\mathbf{e}}_{2\sigma}$	(0.000, 1.000, 0.000)	

$\underline{\mathbf{e}}_{3\sigma}$ (0.000, 0.000, 1.000)

(g)

$\underline{\mathbf{e}}_{1\sigma}$ (1.000, 0.000, 0.000)
$\underline{\mathbf{e}}_{2\sigma}$ (0.000, 1.000, 0.000)
$\underline{\mathbf{e}}_{3\sigma}$ (0.000, 0.000, 1.000)

(h)

$\underline{\mathbf{e}}_{1}$ (1.000, 0.000, 0.000)
$\underline{\mathbf{e}}_{2}$ (0.000, 1.000, 0.000)
$\underline{\mathbf{e}}_{3}$ (0.000, 0.000, 1.000)

References

1. Bader, R.F.W. A Bond Path: A Universal Indicator of Bonded Interactions. *J. Phys. Chem. A* **1998**, *102*, 7314–7323, doi:10.1021/jp981794v.
2. Bader, R.F.W. Bond Paths Are Not Chemical Bonds. *J. Phys. Chem. A* **2009**, *113*, 10391–10396, doi:10.1021/jp906341r.
3. Nakatsuji, H. Common Nature of the Electron Cloud of a System Undergoing Change in Nuclear Configuration. *J. Am. Chem. Soc.* **1974**, *96*, 24–30, doi:10.1021/ja00808a004.
4. Bone, R.G.A.; Bader, R.F.W. Identifying and Analyzing Intermolecular Bonding Interactions in van Der Waals Molecules. *J. Phys. Chem.* **1996**, *100*, 10892–10911, doi:10.1021/jp953512m.
5. Jenkins, S.; Heggie, M.I. Quantitative Analysis of Bonding in 90º Partial Dislocation in Diamond. *J. Phys. Condens. Matter* **2000**, *12*, 10325–10333, doi:10.1088/0953-8984/12/49/3.
6. Ayers, P.W.; Jenkins, S. An Electron-Preceding Perspective on the Deformation of Materials. *J. Chem. Phys.* **2009**, *130*, 154104, doi:10.1063/1.3098140.
7. Jenkins, S.; Morrison, I. The Chemical Character of the Intermolecular Bonds of Seven Phases of Ice as Revealed by Ab Initio Calculation of Electron Densities. *Chem. Phys. Lett.* **2000**, *317*, 97–102, doi:10.1016/S0009-2614(99)01306-8.
8. Jenkins, S.; Maza, J.R.; Xu, T.; Jiajun, D.; Kirk, S.R. Biphenyl: A Stress Tensor and Vector-Based Perspective Explored within the Quantum Theory of Atoms in Molecules. *Int. J. Quantum Chem.* **2015**, *115*, 1678–1690, doi:10.1002/qua.25006.
9. Bader, R.F.W. Quantum Topology of Molecular Charge Distributions. III. The Mechanics of an Atom in a Molecule. *J. Chem. Phys.* **1980**, *73*, 2871–2883, doi:10.1063/1.440457.
10. Anderson, J.S.M.; Ayers, P.W.; Hernandez, J.I.R. How Ambiguous Is the Local Kinetic Energy?†. *J. Phys. Chem. A* **2010**, *114*, 8884–8895, doi:10.1021/jp1029745.
11. Anderson, J.S.M.; Ayers, P.W. Quantum Theory of Atoms in Molecules: Results for the SR-ZORA Hamiltonian. *J. Phys. Chem. A* **2011**, *115*, 13001–13006, doi:10.1021/jp204558n.
12. Xu, T.; Farrell, J.; Momen, R.; Azizi, A.; Kirk, S.R.; Jenkins, S.; Wales, D.J. A Stress Tensor Eigenvector Projection Space for the (H2O)5 Potential Energy Surface. *Chem. Phys. Lett.* **2017**, *667*, 25–31, doi:10.1016/j.cplett.2016.11.028.
13. Wyatt, R.E. *Quantum Dynamics with Trajectories*; Interdisciplinary Applied Mathematics; 1st ed.; Springer: Dordrecht, 2006; ISBN 978-0-387-28145-2.
14. Azizi, A.; Momen, R.; Kirk, S.R.; Jenkins, S. 3-D Bond-Paths of QTAIM and the Stress Tensor in Neutral Lithium Clusters, Lim (m = 2-5), Presented on the Ehrenfest Force Molecular Graph. *Phys. Chem. Chem. Phys.* **2019**, *22*, 864–877, doi:10.1039/C9CP05066C.